HHS Public Access

Author manuscript

Adv Mater. Author manuscript; available in PMC 2017 October 01.

Published in final edited form as:

Adv Mater. 2016 October ; 28(40): 8861–8891. doi:10.1002/adma.201601908.

Glycosaminoglycan-based biohybrid hydrogels: a sweet and smart choice for multifunctional biomaterials

Dr. Uwe Freudenberg[*],

Leibniz Institute of Polymer Research Dresden (IPF), Max Bergmann Center of Biomaterials Dresden (MBC), Technische Universität Dresden, Center for Regenerative Therapies Dresden (CRTD), Hohe Str. 6, 01069 Dresden, Germany

Yingkai Liang,

Department of Materials Science and Engineering and Department of Biomedical Engineering, University of Delaware, Newark, Delaware 19716, United States, yingkai@udel.edu

Prof. Kristi L. Kiick[*], and

Department of Materials Science and Engineering and Department of Biomedical Engineering, University of Delaware, Newark, Delaware 19716, United States and Delaware Biotechnology Institute, 15 Innovation Way, Newark, Delaware 19716, United States

Prof. Dr. Carsten Werner[*]

Leibniz Institute of Polymer Research Dresden (IPF), Max Bergmann Center of Biomaterials Dresden (MBC), Technische Universität Dresden, Center for Regenerative Therapies Dresden (CRTD), Hohe Str. 6, 01069 Dresden, Germany

Abstract

Glycosaminoglycans (GAGs) govern important functional characteristics of the extracellular matrix (ECM) in living tissues. Incorporation of GAGs into biomaterials opens up new routes for the presentation of signaling molecules, providing control over development, homeostasis, inflammation and tumor formation and progression. This review discusses recent approaches to GAG-based materials, highlighting the formation of modular, tunable biohybrid hydrogels by covalent and non-covalent conjugation schemes, including both theory-driven design concepts and advanced processing technologies. Examples of the application of the resulting materials in biomedical studies are provided. For perspective, we highlight solid-phase and chemoenzymatic oligosaccharide synthesis methods for GAG-derived motifs, rational and high-throughput design strategies for GAG-based materials and the utilization of the factor-scavenging characteristics of GAGs.

Keywords

hydrogels; glycosaminoglycans; biomaterials; growth factors; cell-instructive

[*] Corresponding Author, freudenberg@ipfdd.de, werner@ipfdd.de, kick@udel.edu.

1. Introduction

Glycosaminoglycans (GAGs) are unbranched, high-molecular-weight polysaccharides that occur either covalently linked to protein cores—forming proteoglycans—or free within the extracellular matrix (ECM) of higher organisms. GAGs consist of repeating disaccharide units consisting of a uronic acid and an amino sugar that display carboxylic acid and various sulfate moieties (N-sulfate; 2-O-, 3-O-, 4-O-, and 6-O-sulfate).[1] Important types of GAGs that differ in chemical composition, structure and function include the non-sulfated hyaluronan (HA), the sulfated heparan sulfate (HS) and the closely related heparin (HEP), the sulfated chondroitin sulfate (CS) and the related dermatan sulfate (DS), and keratan sulfate (KS). The molecular weights and sulfation patterns of GAGs vary over a broad range, depending on the organism, tissue type, age and health conditions. The physical properties of GAGs, i.e., viscosity and conformation, and interactions with soluble signaling molecules are both strongly influenced by the GAG molecular weight.[2]

GAGs form the structural basis of many important functional characteristics of ECMs. In addition to the hydrogelic properties of tissues (e.g., their compressive resistance),[3] GAGs mediate the localized presentation of multiple soluble signaling molecules,[4] including the formation of morphogen gradients.[5] HS-GAGs, for instance, have been shown to modulate morphogen gradient formation *in vivo*,[6] thus governing the adaptive formation of tissues and organs in multicellular organisms.[7] Accordingly, GAGs have been demonstrated to be involved in key events in embryogenesis and development,[1,8] homeostasis,[8b] inflammation,[9] and tumor formation and progression.[10] In light of the multifaceted cell-instructive roles of GAGs in living tissues, GAG-based materials are currently attracting greatly increased attention in the field of biomaterials science[11] (see **Figure 1**). This review covers recent related developments, highlighting the formation of modular, tunable biohybrid hydrogels using covalent and non-covalent conjugation schemes, including the cytocompatible in situ gelation of GAG-containing polymer networks in biofluids or living tissues (see section 2). In these approaches, GAGs were either conjugated to native structural polymers, such as collagen,[12] or were combined with functionalized synthetic polymers, such as poly(ethylene glycol) (PEG). In particular, the combination of GAGs with PEG has been demonstrated to allow extensive modulation of both the mechanical and biomolecular characteristics of the resulting biohybrid materials (see sections 2 and 5.2).

A variety of related systems has recently been reported and analytically studied with respect to both intrinsic material properties and biological signaling characteristics. The combination of GAGs and functional peptides in biohybrid matrices was demonstrated to provide unprecedented levels of control over crosslinking, cell adhesion and enzymatic cleavage ‘on demand’ (see section 2). Dedicated processing technologies have allowed the adjustment of matrix characteristics across scales (see section 3 and Figure 1), and further customization of the materials was achieved through the non-covalent conjugation of multiple GAG-binding growth factors (see section 4 and Figure 1). Furthermore, selective desulfation approaches have expanded the options for adjusting GAG properties, enabling the unambiguous correlation of molecular structure and cell-instructive matrix characteristics (see section 4.2). Based on their biofunctional versatility, GAG-based materials have been shown to be instrumental for *in vivo* tissue engineering, the culture and

expansion of therapeutically relevant cells, drug delivery applications, and advanced *ex vivo* tissue engineering models (see sections 2-4).

Exciting new features of GAG-based biohybrid materials are now coming into reach because solid-phase oligosaccharide synthesis, in combination with chemical and chemoenzymatic protocols and the recombinant expression of proteoglycans, facilitates the precise design of GAG-derived motifs (see section 5.1). With examples of theory-driven and combinatorial materials design (see section 5.2), approaches to the therapeutically relevant scavenging of GAG-binding cytokines (see section 5.3) and the implementation of autoregulative adaptation schemes (see section 4.4), GAG-based biohybrid materials represent a highly promising new class of bioinspired materials that are capable of addressing the needs of emerging fields such as regenerative medicine and beyond.

2. GAG Hydrogels with Adjusted Stiffness, Cell Adhesiveness and Degradation

GAG-based hydrogel materials can provide cell-instructive molecular signals and allow cell-responsive remodeling. This section discusses approaches for the functionalization of GAG hydrogels with short peptides to trigger cell adhesion and enzymatic cleavage, cytocompatible crosslinking chemistries for embedding living cells and customized degradation schemes to adjust the release of bioactive moieties and the structure of gel materials.

2.1 Multifunctional GAG-Peptide-PEG Hydrogels

2.1.1 Cell-(Responsive) Hydrogel Materials—Cell-fate decisions are controlled by a subtle balance of exogenous cues;[13] thus, ECM-mimicking polymer matrices must be adjusted with respect to mechanical properties and structural heterogeneity, the provision of cell adhesion ligands, susceptibility to cell-responsive remodeling and the delivery of soluble signaling molecules[14] (see Figure 1). In particular, because matrix remodeling is required for the migration and proliferation of embedded cells,[15] cell-responsive degradability is indispensable for cell-instructive matrices in tissue engineering.[14b] Peptide sequences incorporated into GAG-based hydrogels can provide specific adhesion receptor-binding sites and enable cell-responsive remodeling. Accordingly, multifunctional biohybrid hydrogels made of star-shaped PEG (starPEG) and HEP, utilizing 1-Ethyl-3-(3-dimethylaminopropyl)-carbodiimide/N-hydroxysulfoxuccinimide (EDC/sNHS)-activated carboxylic acid moieties of HEP for covalent crosslinking with the amine moieties of the starPEG,[16] were functionalized by incorporation of matrix metalloproteinase-sensitive peptides and specific cell adhesion sites. To allow matrix remodeling, the peptide sequence GPQG-IWGQ, which is sensitive to several matrix metalloproteinases (MMPs), including MMPs 1, 2, 3, 7, 8 and 9,[17] was conjugated to all the arms of a starPEG via a Michael-type addition reaction.[18] The N-terminus of the peptide was subsequently used for oriented coupling to the EDC/sNHS-activated carboxylic acid groups of HEP to form defined biohybrid matrices. In addition, the fibronectin (FN)-derived integrin ligand RGD was incorporated into a bifunctional crosslinking peptide together with the GPQG-IWGQ-sequence.[19] The resulting biohybrid hydrogels, which displayed adhesion sites and enzymatic degradability

within peptide crosslinks pre-functionalized with vascular endothelial growth factor (VEGF), were demonstrated to promote the ingrowth of HUVECs.[19]

The fine-tuning of degradability to adjust the migratory activity of cells can be crucial for the rapid integration of tissue engineering constructs by promoting vascularization and graft integration.[20] Enzymatic degradation was delayed due to the size-dependent exclusion of MMPs from the hydrogel bulk volume but was accelerated by non-specific hydrolytic cleavage, as demonstrated for MMP-sensitive peptides combined with linkers of differing hydrolytic sensitivity in starPEG-HEP hydrogels:[21] MMP-sensitive peptides were linked through either a slowly degrading ester bond or a more stable amide bond to all the arms of the starPEG, which was subsequently converted by HEP-containing covalently conjugated cell-adhesive RGD peptides and complexed with pro-angiogenic VEGF. The ester-linked hydrogel accelerated the enzymatic degradation, the release of VEGF and the ingrowth and *in vivo* vascularization of HUVECs (CAM assay). The hydrogel system allowed variation of the degradation rate for intrinsically invariant material properties (swelling and stiffness) and biomolecular characteristics (RGD concentration and VEGF loading)[21] because only the release of VEGF was directly correlated to the degradation (see section 4.3).

The combination of multiple cell-instructive signals, e.g., the implementation of different adhesion sites, defines an important challenge in attempts to mimic the complexity of the ECM. Additionally, many functional peptides (e.g., IKVAV) contain lysine in their active sequence and thus cannot be linked to GAGs by EDC/sNHS chemistry. Orthogonal conjugation techniques are therefore required for the incorporation of bioactive moieties into gel matrices. Accordingly, a fraction of the carboxylic acid groups of the HEP building block were pre-functionalized with maleimide groups to allow the chemoselective coupling of peptides containing cysteine as a bioinert linker group together with adhesion sequences.[22] This concept allows the subsequent oriented coupling of lysine-containing sequences and was, for example, used to orthogonally couple different RGD peptides (cycloRGDYC, GCWGGRGDSP, and GRGDGWGCG) in a Michael-type addition reaction with the maleimide and the SH group of the peptide's cysteine. It was shown that endothelial cell adhesion (cell density after 7 days) was enhanced in the order cycloRGD > looped RGDSP > linear RGD, which is consistent with earlier findings on the activity of structurally different RGD peptides.[23]

2.1.2 In Situ Gelling Hydrogels for 3D Embedding of Cells—The spatial distribution of matrix cues has been reported to be crucial for the subsequent cellular response.[14a,24] Accordingly, there is increasing interest in materials suitable for the spatiotemporally defined 3D adjustment of biomolecular and physical signals to enable more realistic cell culture experiments *in vitro*[25] and more effective tissue engineering applications *in vivo*. For that purpose, the viscoelastic characteristics, provision of adhesion signals, incorporation of cell-responsive cleavage sites and administration of morphogens must be included in well-defined multicomponent hydrogel matrices (see also section 5.2) to allow the embedding of cells by cell- and tissue-compatible crosslinking schemes. Michael-type addition, copper-mediated azide-alkyne cycloaddition, enzymatic crosslinking, and photo-induced polymerization techniques have been widely explored to embed living cells within 3D polymer matrices.[26] The Michael-type addition reaction is a particular focus

because it provides a fast reaction under physiological conditions, does not require a catalyst or produce side products; therefore, it has been used extensively for the formation of cell-instructive PEG-based hydrogel matrices.[27] This crosslinking reaction was selected to produce well-defined, self-assembling starPEG-peptide-HEP hydrogels.[28] StarPEG-peptide conjugates suitable for self-assembly were produced through a regioselective amino acid protection strategy (see **Figure 2**) in which the protection of the N-terminal cysteine residue with a S-tert-butylthio (StBu) side chain within the applied Fmoc peptide synthesis was followed by purification, PEGylation and deprotection with tris(2-carboxyethyl)phosphine (TCEP).

As such, the procedure described above was used to couple peptides that enabled the binding of cell adhesion receptors (e.g., RGDSP or IKVAV) or cell-responsive remodeling (the MMP-sensitive sequence GPQG-IWGQ; see section 3.1.1) to every arm of a 4-arm PEG. This design prevents defect formation arising from PEG-intramolecular crosslinks and allows the incorporation of water-insoluble, hydrophobic peptides, such as the laminin-1-derived IKVAV. HEP was pre-functionalized through EDC/sNHS-activated carboxylic acid moieties to react with up to eight N-(2-aminoethyl)maleimide molecules. Covalent network formation was spontaneously initiated upon mixing of the starPEG-peptide conjugate with HEP-maleimide, optionally pre-mixed with cells and/or growth factors. Network formation occurred within 30-60 s, and varying the molar ratio of the starPEG-peptide conjugates to HEP (γ) from 0.63 to 1.5 altered the crosslinking degree and therefore caused the storage modulus to vary from 0.2 kPa to 6 kPa. Hydrogels functionalized with GCWGRGDSP or SIKVAVGWCG promoted elongated HUVEC morphology or neurite outgrowth of the dorsal root ganglia. The administration of soluble signaling molecules, such as pro-angiogenic VEGF, SDF-1α or FGF-2, for advanced organoid models is discussed in section 4.3.

HA-based hydrogels crosslinked with dual-cysteine-containing MMP-sensitive peptides utilizing a Michael-type addition were developed by Park and co-workers.[29] Here, acrylated HA of 10 or 50 kDa was crosslinked with GCRDGPQGIWGQDRCG or non-MMP-sensitive GCRDGDQGIAGFDRCG peptides and was additionally functionalized with cell adhesion-mediating RGD peptides with Young's moduli of 0.2-0.4 kPa for the 10 kDa HA and 1.3-1.4 kPa for the 50 kPa HA. The cell spreading of embedded human mesenchymal stem cells (MSCs) required MMP-responsive linkers and was further promoted by the presence of RGD peptides, highlighting the importance of cell-responsive linkers and adhesion cues in controlling cell-fate decisions in GAG-based hydrogel materials.

Multifunctional HEP-containing hydrogels for 3D cellular encapsulation that display tunable mechanical properties and a customized presentation of RGD adhesion peptides or FN were developed by Kiick and co-workers to control the morphology of human aortic adventitial fibroblasts (AoAF).[30] Maleimide-terminated starPEG (4 arms, 10 kDa), thiol-terminated starPEG (4 arms, 10 kDa), maleimide-di-functionalized HEP (f = 2, 3 kDa), cysteine-containing AcGCGYRGDSPG adhesion peptides, and FN were used to form hydrogels in situ via Michael-type addition reaction. The hydrogel design made it possible to systematically study the impact of the presence of the GAG and the RGD adhesion motif:

pure PEG gels modified with RGD (PEG(RGD)), PEG gels modified with low-molecular-weight HEP (LMWHEP) pre-conjugated to RGD (PEG-LMWHEP(RGD)), PEG gels with LMWHEP in which RGD was pre-conjugated to PEG (PEG(RGD)-LMWHEP) and PEG gels modified with LMWHEP in which FN was pre-conjugated to PEG before gelation (PEG(FN)-LMWHEP). The PEG(FN)–LMWHEP gels were prepared with a constant FN concentration but exhibited different mechanical properties (storage moduli of 0.4 and 2.8 kPa). These experiments indicated that hydrogels with higher moduli promoted AoAF adhesion, and improved cellular responses were observed when the RGD motif was chemically attached through linkage to PEG rather than to LMWHEP. Although the synthetic RGD peptide was in 1000-fold excess compared to the native RGD domains of FN in the FN-modified gels, the native environment of FN promoted the best performance in terms of AoAF adhesion and spreading.

Anseth and co-workers developed an adhesion peptide (RGDS)-modified PEG-HEP hydrogel[31] for the 3D encapsulation of human MSCs. PEG dimethacrylate (PEGDM) (optionally pre-functionalized with RGDS peptides) and methacrylated HEP were photocrosslinked using 2-hydroxy-1-[4-(hydroxyethoxy)phenyl]-2-methyl-1-propanone as the photoinitiator. The presence of HEP supported the viability of the embedded human MSCs and promoted their osteogenic differentiation. In an extension of this work, a multifunctional fluvastatin-releasing PEG hydrogel, additionally functionalized with RGDS and HEP, was developed to further promote the osteogenic differentiation of encapsulated human MSCs.[32] Here, the small-molecule drug fluvastatin, which is known for its osteogenic potential, was covalently attached via hydrolytically labile ester bonds made of lactic acid grafted from PEG monomethacrylate. PEG-based hydrogels functionalized with these fluvastatin grafts were formed by photocrosslinking. Optionally, methacrylated HEP and RGD-PEG conjugates were also copolymerized. The fluvastatin-releasing hydrogels were shown to promote the dose-dependent secretion of ALP and BMP-2 by embedded human MSCs. Osteogenic differentiation could be further enhanced by the incorporation of HEP into the multifunctional matrix, which sequestered and therefore localized BMP-2 to the direct cell microenvironment. Altogether, this work is an interesting example of how ECM-mimicking materials provide bidirectional signaling cues: the small-molecule-induced promotion of morphogen secretion by embedded cells is augmented via GAG conjugation and then is further boosted by the osteogenic differentiation of the embedded cells.

Capitalizing on the unique charge pattern of HEP and the fact that most HEP-interacting proteins are conjugated to this GAG via electrostatic interactions, [4a] a similar principle may be utilized to form well-defined physically crosslinked networks. Therefore, a minimal peptide motif for strong interactions with HEP has been developed based on (KA)x or (RA)x repeating units.[33] If the peptides ($x \geq 5$) were conjugated to all four arms of a starPEG, and HEP at a concentration of ≥ 5 mM is mixed with the starPEG-peptide conjugate at a concentration of ≥ 4 mM, hydrogel networks were formed based on physical interactions between the positively charged peptides and the negatively charged HEP. Interestingly, successful hydrogel formation occurred only if the HEP induced α-helix formation in the (KA)x or (RA)x peptides. The gelation time and the stiffness of the hydrogels could be tuned by altering the molar ratio, the total solid content (concentration of the building blocks) and the type of peptide. For instance, hydrogels formed with 5 mM $(KA)_5$ and 5 mM

HEP displayed a storage modulus of ~1.1 kPa, whereas 5 mM $(KA)_7$ and 5 mM HEP formed hydrogels with a storage modulus of ~10 kPa, one magnitude higher. Stability tests of the hydrogels in cell culture medium at 37°C showed an initial burst release of HEP of approximately 20% within the first 9 h, followed by a slow continuous release over 9 days. The encapsulation of human neonatal dermal fibroblasts showed a survival rate of >98%.

This non-covalent crosslinking principle was further utilized to prepare monodisperse starPEG-peptide-GAG microparticles for cell or protein delivery applications.[34] A microfluidic device using a Y-connecter to mix a 3 mM $(KA)_7$-starPEG-peptide conjugate solution and a 5 kDa dextran sulfate solution before 90° injection into a non-miscible oil flow was utilized to produce monodisperse beads with a diameter of 755 ± 28 μm and tunable mechanical properties, such as a storage modulus of ~35 kPa for 20 mM dextran sulfate or ~75 kPa for 7.1 mM dextran sulfate. Optionally, RGD peptides mediating cell adhesion were incorporated within $(KA)_7$-RGDSP-starPEG conjugates. Using these conjugates, the encapsulation of human neonatal dermal fibroblasts with survival rates >98% after 7 days culture was possible; after shock-freezing in liquid nitrogen followed by 6 weeks of storage and re-cultivation, a survival rate of ~86% could be maintained. Thus, these hydrogel beads may be used as delivery vehicles for cell-based therapies.

A similar approach was used to form a multicomponent material via non-covalent interactions between starPEG pre-functionalized with a HEP-binding peptide (CRPKAKAKAKAKDQTK) and HEP-modified HA.[35] The hydrogel material displayed a nanofibrous network structure and was utilized for the proliferation and differentiation of adipose-derived stem cells.

2.2 Advanced Degradation Chemistries

Spurred by recent progress in materials science and polymer chemistry, a wide variety of chemically labile bonds have been exploited to form hydrogels with degradable backbones, crosslinks, and pendant groups.[36] Through selective hydrogel degradation, spatiotemporal changes in matrix properties can be easily achieved, better mimicking the physical and biochemical characteristics of the native ECM and providing tunability of the mass transport and diffusivity of nutrients and encapsulated bioactive molecules.[37] In tissue engineering and 3D cell culture applications, hydrogel degradation plays an important role in inducing cell differentiation, promoting cell secretory properties and controlling the distribution of ECM molecules, which is essential for mimicking the dynamic complexity of the native cellular environment and understanding *in vivo* cell behaviors. In controlled drug and gene delivery applications, hydrogel degradation permits systematic variations in the permeability of the network via engineering of degradation rates and modes, offering excellent opportunities for the on-demand/targeted release of bioactive cargos. Although the field of stimuli-responsive GAG-based hydrogels is still in the early stages, several strategies based on hydrolytic, reduction-sensitive, and light-mediated degradation mechanisms have been developed, as detailed below.

2.2.1 Hydrolytic Degradation—As noted above, the chemical modification of GAGs is usually required to enable subsequent crosslinking for hydrogel formation. Most GAGs are

typically modified at the carboxylic acid groups of their uronic acid residues and the hydroxyl groups of their amino sugar moieties, which usually generates ester linkages that are susceptible to hydrolysis.[38] Despite the non-specific degradation mechanism, the hydrolytic cleavage of ester linkages throughout GAG hydrogels provides a simple approach to introduce temporal changes in network crosslink ing density, which can influence properties such as diffusivity, swelling and mechanics.[37] In addition to HEP, HA is an important building block for the preparation of GAG-based hydrogels owing to its ubiquitous presence in the ECM and its essential roles in a variety of biological processes (e.g., cellular signaling, wound repair, morphogenesis, and matrix organization).[38a,39] Ito and co-workers prepared injectable HA hydrogels via a copper-free click reaction of azide- and cyclooctyne-modified HA.[40] The ester linkages between the HA backbone and the clickable groups allowed the slow degradation of the hydrogels via hydrolysis. Degradation of the hydrogels in PBS was observed in approximately two weeks (i.e., 13-16 days), with a faster degradation rate for hydrogels prepared with lower polymer concentrations. Patterson and co-workers developed degradable HA hydrogels via the photocrosslinking of a glycidyl methacrylate-modified HA (HA-GMA).[41] The degradable properties of the hydrogels were controlled by varying the ratio of high-molecular-weight HA-GMA (220 kDa, fast degradation) to low-molecular-weight HA-GMA (110 kDa, slow degradation) to manipulate the release profiles of BMP-2 and thus enhance bone regeneration in a rat calvarial bone critical size defect model.

However, in many cases, the ester linkages between the HA backbone and the reactive groups are relatively stable due to steric hindrance or a locally hydrophobic environment, resulting in the slow and only partial degradation of the matrix over several weeks.[42] This delay might hinder the diffusion of growth factors, migration of cells, and distribution of ECM proteins. To more systematically control the hydrolytic degradation properties of hydrogels, additional ester linkages can be introduced into GAGs via the incorporation of lactic acid or caprolactone repeats. Burdick and co-workers developed hydrolytically degradable HA hydrogels with different degradation profiles, via the free radical photo-polymerization of various methacrylated HA derivatives, for neocartilage formation.[43] Mixtures of methacrylated HA (MeHA), methacrylated lactic acid HA (MeLAHA) and methacrylated caprolactone HA (MeCLHA) were employed to formulate hydrogels with tunable degradation by varying the proportion of each component. A mixture of MeHA with increasing amounts of hydrolytically degradable MeLAHA was shown to effectively enhance the distribution of ECM molecules released by encapsulated MSCs.[44] In a follow-up study, the temporal properties of the HA hydrogels were modulated by varying the ratio of the components and the overall wt% in the mixture of MeHA and MeCLHA (the more rapidly degrading component). As a result, improved mechanical properties and biochemical content compared to the 1:1 MeHA:MeCLHA hydrogel (overall 2 wt%) were observed over time.[45]

2.2.2 Reduction-Sensitive Degradation—Increased levels of glutathione (GSH), a thiol-containing tripeptide localized to intracellular compartments, are found in both normal and malignant cells and in tumor microenvironments, most likely associated with the cellular proliferative response and cell cycle progression.[46] The incorporation of reduction-

sensitive linkages in hydrogels is thus of significant interest in drug delivery and tissue engineering because hydrogel degradation can be selectively triggered in the presence of reducing species such as GSH, as mentioned above, allowing the targeted release and stimulus-triggered delivery of therapeutic molecules relevant to cancer and wound healing applications. In most cases, reduction-sensitive linkages are incorporated into hydrogels through disulfide bonds, which can undergo rapid cleavage reactions upon exposure to thiol-containing reducing stimuli, leading to matrix degradation.[47] The disulfide-crosslinked GAG hydrogels that are typically generated by the oxidation of free thiols usually lack precisely controlled reaction progress and require a prolonged reaction time (on the scale of hours).[48] Alternatively, Prestwich and co-workers prepared reduction-sensitive, ECM-mimicking hydrogels using disulfide-containing PEG diacrylate crosslinkers and thiol-modified HA and gelatin macromers; these gels were formed in 3 min.[49] These hydrogels degraded rapidly in the presence of N-acetyl-cysteine or GSH, and the encapsulated cells were recovered at both high yields and high viability. Wang and co-workers developed novel disulfide-crosslinked HA hydrogels based on the thiol-disulfide exchange reaction between HA pyridyl disulfide and PEG dithiol.[50] These hydrogels, with tunable mechanical and swelling properties, can be rapidly formed within 4-5 min under physiologically relevant conditions by varying the proportion of the macro-crosslinker PEG dithiol. The disulfide-crosslinked hydrogels exhibited matrix degradation in the presence of GSH via a bulk degradation mechanism, as demonstrated by the measurement of hydrogel mass over time in GSH solutions. Similar disulfide-crosslinked HA hydrogels formed by thiol-modified HA and pyridyl disulfide-modified HA were reported by Ossipov et al., demonstrating complete network degradation within 30 min in the presence of DTT.[51]

Although disulfide-crosslinked hydrogels hold great promise for controlling the release of drugs in GSH-abundant physiological and pathological states, the rapid cleavage kinetics of disulfide bonds (half-lives ranging from 8 to 45 min) could limit the therapeutic effects of the biomolecules encapsulated in these materials. In parallel to the development of disulfide-crosslinked HA hydrogels, Kiick and co-workers recently explored the reversibility of thiol-maleimide Michael-type reactions in the presence of GSH and engineering of the degradation rate of PEG-HEP hydrogels over prolonged time scales (**Figure 3**).[52] Selected thiol-maleimide adducts synthesized from the Michael-type addition were shown to undergo retro and exchange reactions in the presence of GSH, with half-lives ranging from 20 to 80 h (Figure 3A).[53] The rate of the exchange reaction was dependent on the pKa of the Michael donors (thiols), with a lower thiol pKa correlating to an increased rate, which could be used to manipulate hydrogel degradation for the long-term delivery of drugs in reducing environments. PEG-HEP hydrogels with different levels of degradation sensitivity to reducing agents were synthesized by a Michael-type reaction between maleimide-modified HEP and various thiol-functionalized 4-arm PEG polymers (Figure 3B). Tunable degradation of these hydrogels in the presence of GSH was achieved by varying the choice of arylthiol derivatives used to functionalize the PEG polymers. Rheological monitoring of hydrogel degradation revealed rate constants of degradation that were approximately an order of magnitude slower than for hydrogels crosslinked via disulfide linkages. These results suggest the potential of arylthiolether succinimide-containing hydrogels prepared from thiol-maleimide Michael-type reactions to provide alternative options for reduction-

mediated drug delivery over longer time scales than can be afforded by disulfide-linked hydrogels.

Furthermore, the GSH sensitivity of the thiol-maleimide adducts explored in these hydrogels could also be potentially applied to nanogel systems (discussed in section 3.2),[54] permitting the targeted and intracellular delivery of therapeutics with increased blood circulation stability.

2.2.3 Photodegradation—Photocleavable degradation based on photolabile *o*-nitrobenzyl derivatives was pioneered by Anseth[55] and others[56] to engineer photoresponsive hydrogels, which allow real-time manipulation of the physical or chemical properties of materials with precise spatiotemporal control. The photocleavable degradation of hydrogels not only provides excellent opportunities for the photocontrolled, on-demand release of proteins but also offers effective strategies for the temporal and spatial regulation of 3D matrix structures to dictate desired cell functions.[57] In combination with the intrinsic biological activities of GAG molecules, photodegradable GAG-based hydrogels are advantageous in applications ranging from controlled drug delivery to tissue regeneration. Werner et al. recently developed photodegradable hydrogels consisting of HEP- and PEG-peptide conjugates to direct the fate of neural precursor cells (**Figure 4**).[58] By incorporating a photocleavable, *o*-nitrobenzyl amino acid residue in the peptide linker units, the hydrogel matrix can be readily degraded after 2 h of UV irradiation, permitting the facile 3D structuring of a matrix with unique biochemical and mechanical properties. Photopatterning was performed on a multilayer ‘sandwich’ composed of a top photocleavable hydrogel layer, an underlying adhesive RGD peptide layer and a bottom polymer substrate. By utilizing the Micro Lens Array patterning technology, defined channel and well architecture was created within the hydrogel matrix, resulting in the exposure of a surface containing the cell-adhesive RGD peptide within these channels and wells. Neural precursor cells seeded onto these patterned matrices with different spatial confinements (i.e., channel: 1D confinement; well: 2D confinement) demonstrated enhanced cell proliferation compared to cells seeded onto a planar RGD-modified glass surface (0D confinement). Additionally, FGF-2 delivery from the patterned hydrogel matrix exhibited a significant increase in cell attachment and spreading. The work of Werner et al. introduced a novel strategy for combining customized biomolecular functionalization (e.g., the provision of adhesion ligands and growth factors) with spatially defined matrix architecture for the microenvironmental control of stem cells *in vitro*.

More recently, Revzin and co-workers developed photodegradable HEP-based hydrogels for the cultivation and retrieval of embryonic stem cells (ESCs).[59] These hydrogels were formed based on a chemically initiated free radical thiol-ene coupling reaction between thiolated HEP and PEG molecules with bifunctional acryl-terminated photolabile *o*-nitrobenzyl moieties. These HEP-based hydrogels released growth factors in a controlled manner and degraded upon exposure to 365 nm UV light. ESCs cultured on HEP hydrogels incorporating Activin A and FGF-2 exhibited effective differentiation and endodermal gene expression enhanced five- to six-fold compared to control ESCs cultured on glass. Owing to the precise spatiotemporal control of the photodegradation technique, specific stem cell colonies could be selectively retrieved from the same culture dish at different time points to

enable in-dish analysis of stem cell differentiation. Using UV light illumination through a microscope objective, ESC colonies residing on the hydrogels were successfully collected from proximal and distant locations on the same culture dish from day 3 to day 6 for biomarker analysis without disturbing the neighboring cells. These bioactive, photodegradable HEP hydrogels offer a facile and inexpensive approach to characterize the in-dish heterogeneity of the stem cell phenotype without sacrificing hundreds of thousands of cells or losing the microenvironmental context.

3. Microstructured GAG Gels, Nanoparticle-Containing GAG Gels, and GAG Nanogels

GAG-based hydrogel materials can be processed for specific applications, creating structural features at the micrometer and submicrometer scales to maximize interactions with cells. In this section, we describe approaches to the generation of microporous gel materials for enhanced cellular infiltration, nanoparticle-containing gel materials with additional functionality and nanosized gel particles (nanogels) for the intracellular administration of bioactives.

3.1 Macroporous Hydrogels

Physical and structural cues from the ECM are important triggers in controlling cell-fate decisions.[13] Accordingly, GAG-based hybrid materials that incorporate well-defined synthetic polymers to tune the physical properties over a broad range have been reported,[16,60] and the network architecture of these materials could be systematically varied utilizing different molar ratios (e.g., varying crosslinking degree) or different molecular weights of the starPEG and HEP precursors[61] (see **Figure 5** and sections 2 and 5.2). Furthermore, a well-defined macroporous architecture consisting of a complex meshwork of fibrous protein strands might be beneficial to mimic the structural diversity of the ECM, as reviewed in [3]. Creating an interconnecting macroporous network structure can improve cell attachment and migration as well as nutrient, oxygen and metabolite transport.[62] Macroporous hydrogel materials are synthesized utilizing different techniques, such as particle leaching, freeze-drying, gas foaming and electrospinning. Cryogelation (a freeze-drying-based technique) of the biohybrid starPEG-HEP hydrogels allowed the creation of interconnected porosity within these materials[63] (see Figure 5C and D). Here, ice crystals formed by the treatment of an aqueous gel-forming reaction mixture at subzero temperatures acted as a porogen that was subsequently lyophilized, leading to a homogeneous interconnected pore structure with an average diameter of 30-50 μm (see Figure 5D). Cryogels with adhesive RGD peptides promote the attachment, spreading and growth of human umbilical vein endothelial cells (HUVECs).

Nano-indention methods were utilized to characterize the network structure and mechanical properties of cryogels that were found to display unique properties.[64] Due to cryo-concentration effects (freezing of pure ice and therefore concentration of hydrogel precursors), the mesh size of the cryogel struts was much smaller (and the Young's modulus much higher) than in comparable conventional (non-cryo-treated) hydrogels. For example,

Young's moduli for a starPEG-to-HEP molar ratio of 3 were in the range of 1000 kPa (struts) vs. ~6 kPa (bulk), compared to ~30 kPa for conventional hydrogels.

The difference in stiffness range is important for the application of cryogels: the bulk Young's modulus determines the overall physical support of the construct and the surrounding tissue, whereas the microscale Young's modulus of the struts is directly experienced by the cells. Stiff struts provide locally strong guidance signals for cells, comparable to collagen fibrils that exceed the traction forces of steel if normalized to its mass, whereas collagen hydrogels overall display a Young's modulus in the 50-100 Pa range.[65] Accordingly, the macroporous hydrogel provides heterogeneous physical structure signals to the cells, a cue with a tremendous impact on cell growth (e.g., void filling) independent of the initial pore size.[66]

Furthermore, the unique properties of strong local stiffness but bulk compliance lead to high compressibility of cryogel materials: cryogels can be compressed without a significant increase in modulus until the strain is equal to the porosity of the materials (approximately 90%); see [63]. Capitalizing on this unique feature allows applications as a shape-memory material. Therefore, the cryogelation technique was combined with an emulsion polymerization technique to create micrometer-scale cryogel particles that allowed cell growth in the interconnected pores while protecting the cells during injection through a narrow syringe needle for minimally invasive implantation, with the subsequent recovery of the initial size and shape.[67] Cryogel beads were prepared using a water-in-oil emulsion followed by rapid cooling of the mixture to −20°C to allow ice crystal formation and gelation. Subsequent lyophilization led to micropore formation. The cryogel microcarriers were found to be spherical particles with an average diameter of 300 μm and an average pore size of 70 μm (see **Figure 6** A and B). Owing to their high porosity and compressibility, the microcarriers could be injected through a 27G needle (inner diameter of 220 μm) with full recovery of their original shape. Moreover, the microcarriers could be further functionalized with HEP-binding growth factors: glial cell-derived neurotrophic growth factor (GDNF) and nerve growth factor (NGF) could be bound and sustainably released from the matrices (see Figure 6C and D). The functionalized cryogel microcarriers were found to be beneficial for PC12 or MSC pre-cultivation (see Figure 6A) and underwent injection through the 27G syringe with unchanged cell viability, thus demonstrating their applicability as a shape-memory cell transplantation carrier for applications in neurodegenerative diseases.[68]

Another material concept utilizes freeze-drying to produce a macroporous blend of poly(vinyl alcohol) (PVA) and hyaluronic acid (HA) with an average pore diameter of 10-50 μm.[69] Moreover, several approaches use electrospinning to form nanofiber hydrogel meshworks for medicinal applications.[70] HA nanofibers (mean diameter = 200 nm) have been produced from DMF/water mixtures by blowing-assisted electrospinning,[71] and HA blends with gelatin have also been used for electrospinning.[72]

Prestwich and co-workers used thiolated HA derivatives supplemented with poly(ethylene oxide) (PEO) as a leachable diluent to form 3D nanofibrous scaffolds by electrospinning for the cultivation of fibroblasts.[73] In a similar approach, thiolated HA and PEG diacrylate were used in a dual-syringe mixing technique to form electrospun HA scaffolds with an

average fiber diameter of 110 nm.[74] Fibroblasts cultivated within such nanofibrous networks exhibited a dendritic morphology.

Other approaches have used HEP for the functionalization of nanofibrous scaffolds. Degradable cellulose-HEP composite fibers were produced by Linhardt and co-workers utilizing electrospinning techniques.[75] Furthermore, electrospun polycaprolactone fibers have been blended with HEP for controlled GAG release.[76] The scaffolds showed a sustained release of HEP over a period of more than 14 days and could be successfully applied to prevent the proliferation of vascular smooth muscle cells. Accordingly, they might be beneficially applied to prevent stenosis in artificial blood vessels. Moreover, aligned poly(L-lactide) nanofibers functionalized with HEP, FGF-2 and laminin were shown to be beneficial in promoting neurite outgrowth.[77]

3.2 Nanoparticle-Containing GAG Gels

The incorporation of nanoparticles in polymer hydrogel networks provides valuable opportunities for developing nanocomposites with tailored physical properties and custom-made functionalities.[78] Such hybrid systems not only allow for introducing structural diversity, but also offer additional handles for engineering multifunctional properties that improve function, including improved mechanical strength, controlled release profiles, and stimuli-responsiveness.[79] Nanoparticle-containing hydrogels integrate two distinct material platforms into one robust hybrid system with unique physical and chemical properties that are absent in the individual building blocks. Motivated by these advantages, a number of recent studies was dedicated to the incorporation of nanoparticles, especially metallic nanoparticles, into GAG-based hydrogels to afford antimicrobial protection, enable imaging/targeting, provide mechanical reinforcement, and self-healing.

The need for GAG-based materials with antimicrobial properties is motivated by the fact that bacterial infection is among the most serious problems for implant materials in contact with blood.[80] Accordingly, thrombin-cleavable starPEG-HEP coatings with incorporated silver nanoparticles[81] were established on top of a thermoplastic polyurethane material commonly used for the fabrication of cardiovascular catheters. The first layer of starPEG-HEP gels contained embedded silver nanoparticles stabilized by interactions with the negatively charged sulfate groups of HEP. This layer was subsequently covered with a non-silver-loaded starPEG-HEP hydrogel to slow the release of the silver nanoparticles and improve blood compatibility. This multilayered hydrogel exhibited long-term antiseptic efficacy against *Escherichia coli* and *Staphylococcus epidermidis* strains *in vitro* and superior performance in the human whole-blood assay with respect to hemolysis, platelet activation and plasma coagulation. Similarly, iron oxide nanoparticles have been incorporated into HA hydrogels as magnetic resonance imaging (MRI) contrast agents. Ossipov and co-workers[82] have developed multifunctional HA hydrogels composed of iron oxide nanoparticle hybridized HA nanogels utilizing a chemoselective hydrazone coupling reaction. Upon the enzymatic degradation of hydrogels by hyaluronidase, the release of nanogels led to a decrease in the concentration of iron oxide nanoparticles within the matrix, which allows the real-time monitoring of hydrogel degradation via MRI. Additionally, the rate of network degradation also provides insight on the pharmacokinetics of the

encapsulated drugs within the nanogels. These iron oxide nanoparticle-containing HA hydrogels thus provide a promising theranostic tool for the monitoring of hyaluronidase-mediated delivery of therapeutic molecules as well as the imaging and recognition of the hydrogel degradation after implantation.

In addition to the physical incorporation of nanoparticles in GAG matrices, metallic nanoparticles have also been employed as multifunctional crosslinkers to formulate GAG hydrogel nanocomposite. Gabilondo and co-workers[83] have covalently immobilized maleimide-functionalized silver and gold nanoparticles into hydrogels based on gelatin and CS via the maleimide-furan Diels-Alder cycloaddition. The resulting nanoparticle-crosslinked hydrogels exhibited increased mechanical strength, with storage modulus values (~18-20kPa) that are nearly three times higher than those of the control hydrogels lacking nanoparticles (~6-7kPa), indicating the formation of a more robust crosslinked network via nanoparticle-crosslinking strategies. On the other hand, Prestwich and co-workers[84] have developed dynamically crosslinked gold nanoparticle-HA hydrogels based on the well-known interaction of gold surfaces with thiolated biomacromonomers including HA and gelatin (**Figure 7**). The soft nature of the hydrogels (~200Pa) and the reversible and dynamic gold nanoparticle-thiol crosslinking allows the development of extrudable bioprinting materials that can form and reform during and after the printing process. The gold nanoparticle-HA hydrogels were then used to print tubular tissue constructs using an automated bioprinting system. The fibroblast-containing constructs were cultured for 4 weeks, after which matrix remodeling and secretion of an endogenous collagen-rich ECM were observed. This study presents a novel strategy in bioprinting with the use of gold nanoparticles as multivalent crosslinkers, offering additional opportunities for building complex tissues in tissue engineering.

3.3 Nanogels

Owing to the increasing impact of nanotechnology on the development of nanoscale delivery vehicles and devices over the past several decades, a wide variety of polymeric nanoparticles have been developed, including polymer-drug conjugates,[85] block copolymer micelles,[86] and polymer nanogels.[87] These polymeric nanostructures (10-150 nm) not only can penetrate vessels and accumulate in specific tissues (e.g., tumors) but also can be functionalized with specific ligands for targeting effects, thus providing a promising platform for nanoparticle therapeutics.[88] In particular, crosslinked polymer nanogels have attracted significant attention in recent years. Composed of crosslinked hydrophilic polymer chains, nanogels maintain high structural integrity even under dilute conditions, with an excellent capacity for the encapsulation of bioactive molecules, suggesting significant potential for the delivery of a wide variety of therapeutic molecules, including chemotherapeutics,[89] proteins,[47a,90] and siDNA.[91]

With the growing appreciation and exploitation of the unique biological and physicochemical properties of GAGs, various GAG-based nanogels have attracted increased interest because of the advantages arising from their nanoscale dimensions and biological activities.[92] For example, the high-affinity binding of HEP to many angiogenic growth factors has been advantageous in preventing burst release from these nanocarriers.[93] In

addition, HA can target the cluster determinant 44 (CD44) receptor, a cellular receptor that is often overexpressed in many types of cancer cells.[39a] CS also shows strong binding affinity to CD44 receptors and demonstrates prolonged circulation in the body.[94] To construct GAG-based nanoplatforms for drug delivery, chemical modifications of the hydrophilic GAGs are necessary to allow either the supramolecular or covalent crosslinking of the molecules. Interested readers are also directed to other recent reviews on more specific applications of various GAG nanogels.[92,93,95]

3.2.1 Physically Crosslinked GAG Nanogels—Nanogels formed by physical crosslinking generally involve the assembly and/or aggregation of macromolecules based on various physical interactions, including hydrogen bonding, electrostatic attraction, and hydrophobic interactions.[96] Physical crosslinking strategies avoid the addition of any chemical crosslinking reagents that might cause undesired interactions with or chemical modification of the encapsulated therapeutic molecules. Moreover, the physical crosslinking of nanogels is performed in mild and mostly aqueous preparation conditions, avoiding the adverse effects that may occur with the use of organic solvents. Among various physical crosslinking mechanisms of GAG-based nanogel formation, hydrophobic interactions have been commonly employed, which involve the chemical modification of the hydrophilic GAGs with hydrophobic moieties and polymers. The inherent amphiphilicity of the hydrophobically modified GAGs provides a driving force for the assembly of these macromolecules into percolated nanogels. A wide variety of studies have generated such nanogels, and the most recent work is summarized below.

HEP-Pluronic® nanogels (~90 nm in diameter) were previously developed for the delivery of chemotherapeutics (e.g., RNase A, DNase and paclitaxel) by covalently conjugating pluronic® F127 to a HEP backbone via EDC/NHS coupling chemistry.[97] Ribonuclease A (RNase A) was incorporated into the HEP–Pluronic® nanogels during nanogel formation via electrostatic interactions. These nanogels exhibited a high loading efficiency of RNase A (>78%) and were efficiently internalized into HeLa cells, where they were localized to the cytosol and the nucleus. Subsequently, these HEP-Pluronic® nanogels were used as multidrug nanocarriers via the simultaneous encapsulation of deoxyribonuclease (DNase) and paclitaxel for combination chemotherapy.[98] The evaluation of the nanogel-treated HeLa cells via the MTT assay demonstrated that the combined delivery of DNase and paclitaxel by the nanogels exhibited a dose-dependent synergistic cytotoxicity compared to the effects of single-drug and free-drug treatments.

More recently, these HEP-Pluronic® nanogels have also been exploited as carriers for both protein and gene delivery to promote neovascularization in tissue engineering applications.[99] By taking advantage of HEP-protein interactions, HEP-Pluronic® nanogels allowed the binding and encapsulation of basic fibroblast growth factor (FGF-2). FGF-2 was released from the nanogels in a slow and sustained manner, with only ~20% release in 2 days, confirming that the majority of the growth factor remained in the nanogels when they were delivered to the cells. The negatively charged nanogel surface was then coated with cationic polyethylenimine (PEI), allowing subsequent complexation with plasmid DNA (pDNA) encoding vascular endothelial growth factor (VEGF). The measured transfection efficiency of the VEGF gene from the nanogels in human endothelial progenitor cells

(EPCs) was 35% in 2 days, with significantly higher expression of VEGF protein in EPCs than from the control nanogel with not VEGF gene complexation. Supramolecular nanogels encapsulating FGF-2 and complexed with the VEGF gene were shown to effectively induce the differentiation of human EPCs into endothelial cells and promote vascular formation in both Matrigel and a mouse model of limb ischemia.

Likewise, HA has also been modified to mediate its assembly into nanogels in aqueous solutions. Akiyoshi and co-workers developed HA-based anionic nanogels (20-70 nm in radius) based on the assembly of cholesteryl groups bearing HA for protein delivery.[100] The resulting HA nanogels demonstrated efficient binding to various types of proteins without denaturation, such as recombinant human growth hormone (rhGH), erythropoietin, exendin-4, and lysozyme. Using the NaCl-induced association of HA nanogels, an injectable hydrogel was formed and employed for the sustained release of rhGH in rats for over a week. Similarly, cholesterol-modified HA nanogels have been covalently conjugated to various small-molecule drugs (etoposide, salinomycin and curcumin) and enzymes (bovine serum amine oxidase) to improve the therapeutic efficacy of chemotherapies.[101] In addition to cholesterol, thermoresponsive polymers have been used as triggerable hydrophobic modifications of GAGs. Auzély-Velty and co-workers modified HA with a thermosensitive copolymer prepared from diethyleneglycolmethacrylate (DEGMA) and oligoethyleneglycolmethacrylate (OEGMA) (**Figure 8**).[102] The thermosensitive HA derivatives were shown to assemble into spherical gel particles above the lower critical solution temperature of the polymer (LCST, 34-35°C), allowing the facile encapsulation of therapeutic molecules. These thermoresponsive HA nanogels were employed as carriers for paclitaxel (cancer drug) and distyrylbenzene derivatives (hydrophobic dyes). The nanogels showed enhanced potency and selectivity in the eradication of CD44-positive human ovarian cancer cells and achieved successful delivery of the dye to macrophages *in vitro* and to macrophages of hepatic and splenic tissues in mice. These systems may thus have significant potential for targeted chemotherapies and the treatment of liver and spleen macrophage-associated diseases.

In a similar approach, CS was hydrophobically modified with acetic anhydride[94b,103] and methacrylamide[104] to form self-assembled CS nanogels in aqueous solutions, which demonstrated efficient internalization in HeLa cells via CD44-based targeting in cancer therapy and the sustained release of transforming growth factor-β (TGF-β) via electrostatic interactions in tissue engineering.

3.2.2 Chemically Crosslinked GAG Nanogels—Although physically crosslinked nanogels offer mild preparation conditions without the use of crosslinking agents, they usually suffer from a lack of long-term stability when circulating in the bloodstream.[96] In contrast, nanogels formed via chemical crosslinking can maintain colloidal stability under dilute *in vivo* conditions, preventing the premature leakage of encapsulated molecules via the unwanted dissociation of the hydrogel network.[105] Many covalent crosslinking strategies, including radical polymerization, step-growth polymerization, photo-polymerization, and thiol-disulfide exchange, have been widely exploited in nanogel synthesis.[96]

The incorporation of chemically labile linkages allows the covalently crosslinked structure of these nanogels to undergo degradation in response to certain stimuli,[106] enabling the on-demand or targeted release of therapeutic molecules and clearance of the carriers from the body upon completion of the delivery.

Typically, chemically crosslinked GAG-based nanogels have been synthesized under dilute conditions based on the crosslinking reactions of water-soluble GAG molecules modified with reactive functional groups, such as vinyl and thiol groups.[107] Jiang and co-workers prepared HA nanogels (*ca.* 70 nm in diameter) based on the radical copolymerization of methacrylated HA and di(ethylene glycol) diacrylate in complete aqueous solutions.[108] These HA nanogels demonstrated great tumor-penetrating capacity and improved antitumor efficacy in both two-dimensional (2D) cultivated cells and three-dimensional (3D) multicellular spheroids *in vitro* and in a subcutaneous hepatic H22 tumor-bearing mouse model. GAG nanogels with well-controlled nanostructures can be obtained by inverse emulsion polymerization methods in which the polymerizable precursors are confined within water-in-oil nanoemulsion droplets as nanoreactors, permitting the isolated crosslinking of each droplet and the facile incorporation of bioactive molecules.[90,109] Jia and co-workers synthesized HEP-decorated, HA-based hydrogel particles (1.1 μm and 70 nm in diameter) crosslinked by divinyl sulfone using an inverse emulsion polymerization technique.[110] Taking advantage of the growth factor-binding affinity of HEP, these hydrogel particles demonstrated a high loading capacity (173-186 ng/mg particles) for bone morphogenetic protein-2 (BMP-2) and released the BMP-2 protein in a controlled manner, with 5-76% release over 13 days, depending on the HEP content of the hydrogel particles. Similarly, McDevitt and co-workers developed HEP microparticles (~5.6 μm in diameter) using a water-in-oil emulsion system and demonstrated the sustained release of bioactive BMP-2 from these carriers for over 28 days.[111] Additionally, Xi and co-workers reported the facile preparation of CS nanogels based on the free radical polymerization of maleoyl-acylated CS in a hexane/water inverse emulsion system.[112] The hydrodynamic diameter (145-340 nm) and release characteristics of these CS nanogels could be systematically controlled by tuning the degree of maleoyl substitution. In a more recent study, Ravaine and co-workers synthesized well-defined HA nanogels comprising methacrylate-modified HA using free radical photopolymerization in inverse nanoemulsions.[113] The crosslinking densities of these nanogels could be controlled not only by the photopolymerization conditions (i.e., the duration and intensity of UV irradiation) but also by the degree of methacrylation of HA. These HA nanogels exhibited good compatibility when incubated with murine 3T3 fibroblasts and demonstrated high stability during one month of storage at 4°C.

Although the facile incorporation of bioactive molecules into nanogels can be easily achieved by inverse emulsion polymerization methods, the required use of organic solvents in the formation of the emulsions can be detrimental to the therapeutic cargo. Alternatively, nanogels have been prepared using nanotemplates (e.g., liposomes) as nanoscale reaction vessels,[54,114] which largely avoided the use of organic solvents during synthesis and generally permitted better control over the size of the resulting nanogels. Auzély-Velty and co-workers developed HA nanogels based on the thiol-ene reaction between pentenoate-modified HA and PEG-bis-thiol using liposome templates (**Figure 9**).[115] The HA and PEG

precursors were encapsulated in the aqueous lumen of the liposome, and unencapsulated precursors were removed by centrifugation. These precursor-containing liposome suspensions were then exposed to UV light to trigger the crosslinking reaction. HA nanogels (~344 nm in diameter) were obtained upon the removal of the lipid template using sodium cholate, an ionic detergent commonly used for lipid membrane solubilization. The monodisperse distribution and spherical structures of these nanogels were confirmed via TEM and SEM. This work presented a facile approach for the formation of GAG nanogels with uniform networks and tunable swelling properties under mild physiological conditions, offering an excellent platform for the development of nanoparticle therapeutics.

Although the stability of crosslinked nanogels in the bloodstream is essential, the selective disassociation of the nanogel crosslinks at the disease site is highly desirable to achieve the targeted delivery of the encapsulated therapeutic molecules upon degradation, which enhances therapeutic efficacy and reduces toxic side effects. A variety of strategies based on cleavable covalent linkages have been used to achieve the triggered release of therapeutic agents from nanogels in response to environmental stimuli, including pH, light, redox potential, and enzyme activity.[96]

Among these stimuli-responsive strategies, reduction-sensitive linkages based on disulfide crosslinks have been employed in the synthesis of stimuli-responsive GAG nanogels. Disulfide bonds are known to undergo rapid cleavage in the presence of GSH, a thiol-containing tripeptide localized to cellular compartments or overproduced in tumor microenvironments.[116] Given the greatly increased concentration of GSH in intracellular compartments or tumor tissues (ca. 0.5–10 mM in cells/tumors vs. 10 μM in circulation),[117] these disulfide-crosslinked nanogels remain stable during circulation in the blood and undergo rapid degradation once they are internalized in cells or localized in tumors, thus enabling the site-specific delivery of anti-tumor drugs. In the earliest studies of disulfide-crosslinked GAG nanogels, Park and co-workers developed disulfide-crosslinked HA nanogels and HEP nanogels for the intracellular delivery of green fluorescent protein (GFP) siRNA and the GSH-triggered release of free HEP to induce apoptotic cell death, respectively.[118] Similarly, Park and co-workers prepared reduction-sensitive HEP-Pluronic® nanogels via the disulfide crosslinking of thiolated HEP-Pluronic® copolymers.[119] These nanogels exhibited a high loading efficiency of positively charged RNase A (~80%) with GSH-mediated release profiles of the protein *in vitro*. Gama and co-workers synthesized disulfide-crosslinked HA nanogels via a thiol-disulfide exchange reaction between thiolated HA and a bifunctional pyridyl disulfide crosslinker, demonstrating increased stability upon dilution compared to noncrosslinked assembled nanostructures and rapid disintegration upon treatment with DTT.[120] More recently, Jiang and co-workers reported the facile synthesis of reduction-sensitive HEP nanogels (80-200 nm in diameter, depending on crosslinking density and reaction time) via the radical copolymerization of methacrylated HEP and disulfide-containing cystamine bisacrylamide in an aqueous medium.[121] The HEP nanogels exhibited strong reduction-sensitive release behavior of DOX *in vitro* and showed remarkable accumulation in tumors of hepatic H22 tumor-bearing mice, suggesting the significant potential of these nanogels as tumor-targeted delivery vehicles for cancer therapeutics and diagnostics.

4. GAG Hydrogels as Tunable Release Systems

Similar to other gel materials, GAG-based gels can entrap therapeutically relevant molecules for localized delivery. Furthermore, the affinity of GAGs for many potent bioactives can be exploited in the design of gel systems that enable localized long-term bioactive administration. GAG hydrogels that use both principles for sustained release applications are described below.

4.1 Entrapment

Because of their excellent compatibility, non-immunogenic nature and unique biological functions, HA hydrogels have been extensively employed as carriers for molecule delivery applications. Because HA is the only non-sulfated member of the GAG family, most therapeutic molecules are sterically entrapped in HA hydrogels without specific binding affinity. A wide variety of molecules, including small-molecule drugs, proteins, and nucleotides, have been entrapped in HA hydrogels to promote tissue repair, cell migration, morphogenesis and matrix remodeling.

4.1.1 Physically Crosslinked HA Hydrogels—Physically crosslinked hydrogels formed by supramolecular interactions exhibit viscous flow under shear stress and rapid recovery when the applied stress is relaxed. This advantageous shear-thinning property permits the facile injection of hydrogels and the local delivery of therapeutic molecules. In a recent example, Burdick and co-workers designed injectable HA hydrogels based on the guest-host interactions of adamantine-modified HA (Ad-HA) and β-cyclodextrin-modified HA (CD-HA) (**Figure 10**).[122a] The tunable release of bovine serum albumin (BSA) from these self-assembling HA hydrogels for up to 60 days was achieved by varying the macromer concentration and the extent of adamantine modification.[115a] In addition to tuning the diffusive release kinetics of biomolecules through variations in crosslinking density, the controlled release of therapeutics (especially small molecules) can be achieved via inclusion effects with the CD moieties in these hydrogels. In a follow-up study, the affinity of CD-HA for small molecules was leveraged to tune the release of tryptophan-modified peptide (model drug), doxorubicin (chemotherapeutic) and doxycycline (MMP inhibitor) from the assembled hydrogels.[122b] Sustained release of these small molecules was observed for up to 21 days, with tunable release profiles that were dependent on CD concentration and drug-CD affinity. These systems provide a minimally invasive injectable platform for the tunable and controlled release of both biomolecules and small-molecule drugs.

4.1.2 Chemically Crosslinked HA Hydrogels—Chemically crosslinked hydrogels formed by covalent bonds not only provide a more stable network structure with increased mechanical strength but also offer great versatility in controlling network degradation and introducing/releasing biological cues (e.g., cell adhesion peptides and growth factors). Chemically crosslinked HA hydrogels are usually formed via the covalent crosslinking of HA derivatives modified with reactive groups, such as thiols, acrylates, aldehydes, hydrazides, and tyramine. These HA hydrogels have been widely used as delivery vehicles for the steric entrapment and controlled release of various bioactive factors, such as

dexamethasone to treat rheumatoid arthritis,[123] BMP-2 to promote bone regeneration,[124] VEGF and FGF-2 to stimulate localized microvessel growth,[125] and DNA to guide cellular processes involved in tissue regeneration and repair.[126]

To minimize the initial burst effect and further prolong the release process, especially for growth factors (considering their high cost), hierarchically structured HA hydrogels containing drug/protein-loaded particles were developed. Burdick and co-workers demonstrated the controlled local delivery of TGF-β with release times extending up to 6 days from alginate microspheres within HA hydrogels, resulting in enhanced MSC chondrogenesis.[127] Jia and co-workers covalently integrated BMP-2-loaded HA microgels into macroscopic HA networks via photocrosslinking, providing zero-order release of the growth factor over 13 days.[128]

Subsequently, dexamethasone-loaded micelles were also covalently integrated into these HA hydrogels as drug depots, offering sustained release over an extended period and mechanically triggered release characteristics.[129] Other strategies, including the incorporation of HEP/HEP mimetics[130] and synthetically sulfated HA polymers[131] into the HA hydrogels, have been developed to sequester growth factors and prolong their release. These tunable release systems based on electrostatic interactions will be discussed in detail below.

4.2 Electrostatic Conjugation/Release

GAGs are linear molecules that—with the exception of the non-sulfated HA—display a characteristic pattern of strongly acidic sulfate groups along the carbohydrate backbone.[4b] Geometrically matching the electrostatic interactions between these sulfate (and carboxylate) moieties and the positively charged amino acid residues of proteins can govern transport, information transfer, and metabolism and therefore direct cell-fate decisions and tissue development.[8b] Accordingly, engineered matrices containing sulfated GAGs can capitalize on the electrostatic binding and redistribution of a wide variety of functional proteins.[11,93,131b,132] Related approaches are summarized below.

4.2.1 Multifunctional Hydrogels for Sustained Factor Release—The GAG HEP is the biomolecule with the highest charge density known in nature and therefore has a high affinity for a variety of proteins.[4a] Based on this property, we developed a biohybrid hydrogel utilizing HEP as a major building block together with star-shaped PEG to form cell-instructive hydrogel matrices.[16] The high HEP concentration of the hydrogel allows the efficient administration of HEP-affine growth factors, such as FGF-2,[16] VEGF,[133] BMP-2,[134] SDF-1α,[135] GDNF,[136] NGF,[67] and TGF-β,[137] as well as the less-affine EGF.[138] Due to the high HEP concentration (i.e., the high number of protein-binding sites) in HEP-based hydrogels, multiple factors can be independently administered, as was shown for the parallel release of FGF-2 and VEGF[139] as well as FGF-2 and GDNF.[136] Accordingly, hydrogels can be used as an adaptable release system for different target tissues. Related applications will be discussed below, including new treatments for neurodegenerative disorders, the stimulation of angiogenesis, the treatment of kidney diseases and the improvement of dermal wound healing. Furthermore, similar applications

of HEP-functionalized hydrogel matrices will be discussed (see also section 4.3 and **Figure 11**)

StarPEG-HEP hydrogels were introduced to explore new options for the treatment of neurodegenerative disorders, such as Parkinson's disease, a disorder characterized by the degenerative loss of dopaminergic neurons.[140] Accordingly, hydrogels were designed to create an optimal niche for this particular cell type to promote cell replacement therapies.[68] As such, starPEG-HEP hydrogels functionalized with RGD peptides and FGF-2 were used to promote the differentiation and survival of dopaminergic neurons.[16] This concept was further developed using RGD-modified starPEG-HEP hydrogels that released a combination of FGF-2 and GDNF to trigger the differentiation and axodendritic outgrowth of dopaminergic neurons derived from primary murine midbrain cells.[136] Shape-memory microscale macroporous hydrogels that released GDNF and NGF, allowing minimally invasive injection through a narrow 27-gauge needle, were successfully utilized to cultivate human MSCs and neuronal PC12 cells, showing their potential as survival-boosting cell-transplantation carriers for Parkinson's disease[67] (see also section 3). Overall, this biohybrid material seems to be an adaptable platform suitable for applications in neurodegenerative disorders.[68]

Because of limited diffusive oxygen transport in mammalian organisms, angiogenesis (the growth of blood vessels from pre-existing vessels) is essential for organ development, growth, and regeneration and thus for every tissue engineering construct transplanted into the body.[141] Accordingly, angiogenesis-supporting materials have been a focus of tissue engineering and biomaterial research in recent years. Although key players such as the pro-angiogenic growth factors VEGF and FGF-2 have been successfully applied to promote angiogenesis in animal models, no clinical breakthrough has yet occurred, which is partially attributed to inefficient growth factor delivery.[141] StarPEG-HEP hydrogels were optimized for the sustained delivery of FGF-2 and VEGF for more than one week through variation of the mechanical properties of the gels,[133] allowing the decoupling of biophysical and biomolecular signaling characteristics according to the rational design principle of this type of hydrogel (see section 5.1). The release of both factors was further independently tuned by variation of the initial loading concentration, which relied on the high density of binding sites within the HEP-based matrices.[139] The simultaneous release of both FGF-2 and VEGF from starPEG-HEP hydrogel matrices was demonstrated to be beneficial in promoting the pro-angiogenic response of HUVECs and vascularization at the chorioallantoic membrane of fertilized chicken eggs (CAM assay).

As outlined above (see section 4.1), HA-based hydrogels have been used extensively for the entrapment of growth factors. Extending this concept, Prestwich and co-workers developed an HA-gelatin-PEG hydrogel that was systematically doped with 0.03%, 0.3% and 3% of a 15 kDa HEP to incorporate this highly sulfated GAG as an affinity center for specific interactions with the pro-angiogenic factors FGF-2 and VEGF.[142] All the building blocks (HA, gelatin and HEP) were thiolated and then crosslinked with PEG diacrylate via a Michael-type addition, and FGF-2 and VEGF were premixed before crosslinking. The presence of HEP within the multifunctional hydrogels caused a stepwise decrease in the released amount of VEGF, clearly showing the tremendous effect of specific interactions

with highly sulfated HEP. Similar effects were shown for FGF-2, but compared to pure HA gels (without HEP), the release was significantly higher—a result explained by the stabilizing effect of HEP, which prevents the thiol moieties of FGF-2 from reacting with PEG diacrylate. However, the investigated hydrogels with variable growth factor functionalization were only partially effective in the stimulation of angiogenesis *in vivo*.

Wang and co-workers recently developed an injectable hydrogel based on two types of physical bonds: host-guest chemistry and electrostatic interactions to form non-covalent bonds between mono-carboxylic acid terminated PEG grafted with poly(ethylene argininylaspartate diglyceride), α-cyclodextrin and heparin.[143] The shear thinning hydrogel was used to incorporate FGF-2 via electrostatic interactions to heparin and interestingly an almost linear release kinetics going parallel with hydrogel degradation was found over a time period of 16 days. Acute toxicity of the material could be excluded performing toxicity assays with primary baboon arterial smooth muscle cells. Altogether, the material might be used as injectable drug release system for heparin affine signal molecules.

Morphogen gradients are ubiquitous in development and regeneration but are often observed to be insufficient under pathologic conditions.[7a] The GAG-mediated release of chemoattractant molecules over prolonged time periods can help to overcome the resulting limitations by forming stable gradients to redirect cell migration and enforce the recruitment of pro-regenerative cells. As a striking example, recovery after myocardial infarction is limited by the insufficient regeneration potential of cardiomyocytes.[144] However, potent chemoattractants, such as SDF-1α, have been shown to direct pro-regenerative stem and progenitor cells, such as early EPCs, to ischemic sites.[145] StarPEG-HEP hydrogels were accordingly used to generate SDF-1α gradients to attract circulating pro-angiogenic cells.[135] The release of SDF-1α was found to be adjustable through the choice of loading concentration (see Figure 11B) and by MMP-mediated hydrogel cleavage. *In vitro* studies confirmed that the migration of EPCs toward concentration gradients of hydrogel-delivered SDF-1α was significantly enhanced. The feasibility of this concept was confirmed *in vivo*: subcutaneously transplanted SDF-1α-releasing hydrogels caused a massive infiltration of EPCs (see Figure 11C) and improved vascularization. In the next step, the guiding properties of the hydrogels were further improved by functionalization using an engineered SDF-1α variant that was activated upon contact with the inflammation-associated protease dipeptidyl peptidase-4 (DPP-4).[146] The enzymatic activation of this chemoattractant resulted in a significant increase in EPC migration.

Multifunctional starPEG-HEP hydrogels were further applied for the sustained delivery of growth factors to treat acute kidney injury (AKI).[147] Hydrogel-delivered FGF-2 and EGF were shown to promote tubular proliferation in experimental AKI in mice.[138] In this system, the strongly HEP-binding FGF-2 displayed sustained release from starPEG-HEP hydrogels (~6% of the loaded amount after 96 h), whereas EGF, which lacks specific binding sites and undergoes unspecific electrostatic interactions with strongly negatively charged hydrogels only,[148] was found to exhibit approximately 10-fold higher release rates (~60% of the loaded amount after 96 h). Nonetheless, the release of both factors had a positive effect in AKI mice.[138] FGF-2-releasing hydrogels induced significantly higher proliferation of tubular epithelial cells in the kidney, and EGF-releasing gels induced a

significant effect on proliferation at a rather low (50 ng) dose compared to previous studies that required a 20 μg dose of EGF.[149]

Wound healing is a dynamic process that can be divided into three phases—inflammation, tissue formation, and tissue remodeling—which are controlled by a complex interplay of soluble mediators, blood and parenchymal cells as well as exogenous cues from the ECM.[150] Accordingly, there are several therapeutic concepts for treating wound healing disorders through the localized delivery of soluble growth factors, such as PDGF, FGF-2 or VEGF. To overcome the rapid inactivation or clearing of soluble mediators from the wound site, the localized and sustained release of such factors would be beneficial. Prestwich and co-workers utilized hydrogel films formed of co-crosslinked thiolated derivatives of chondroitin 6-sulfate (CS) and HEP with PEGDA for the controlled release of FGF-2 to full-thickness wounds in genetically modified diabetic (db/db) mice.[151] Hydrogels consisting of CS-PEGDA and CS-HEP-PEGDAP with different loadings of FGF-2 were compared, and a stepwise increase in wound closure from CS-PEGDA to CS-HEP-PEGDA and increasing amounts of loaded FGF-2 was observed. Thus, incorporation of HEP into hydrogel matrices was concluded to be beneficial for the sustained release of active growth factors, such as FGF-2. In another approach to improved dermal wound healing, the previously mentioned starPEG-HEP hydrogels were successfully utilized for the sustained release of TGF-β to induce myofibroblast differentiation.[137]

4.2.2 Tuning of GAG Sulfation Patterns to Modulate Morphogen Release—The sulfation pattern of GAGs determines their affinity for proteins and therefore the stability of GAG-protein complexes, which in turn influences the transport processes and activity of these signaling molecules within the ECM.[4b] The anticoagulant activity of HEP, for instance, is dependent on a well-defined pentasaccharide sequence involving the relatively rare 3O-sulfate.[152] Accordingly, the selective removal of this particular sulfate moiety can effectively dampen the anticoagulant activity of HEP, for example, to prevent the hemorrhagic side effects of HEP matrices.

Capitalizing on previously established protocols for the regioselective removal of sulfate groups from sulfated carbohydrates such as HEP,[153] the starPEG-HEP hydrogel platform was extended to systematically adjust the affinity of the gels for soluble signaling molecules via the removal of N-sulfate, 6O-sulfate or 2O-sulfate groups from HEP.[154] All reaction schemes for hydrogel crosslinking involve the carboxylic acid groups of HEP; therefore, desulfation not only influences the uptake and release of signaling molecules but directly influences the reactivity of the carboxylic acid group and therefore the network formation. Accordingly, the rational design concept was extended to adjust the mechanical properties of hydrogels made of differently desulfated HEPs (for details, see section 5.1), ultimately enabling the formation of hydrogels with similar mechanical properties but entirely different sulfation patterns. These hydrogels exhibited an average of ~3 (standard HEP, SH), ~2 (N-desulfated HEP, N-DSH), ~1 (6O- and N-desulfated HEP, 6O+N-DSH) and ~0.3 (completely desulfated HEP, cDSH) sulfate groups per disaccharide unit, which altered the release of FGF-2 after 96 h.[154]

Next, the influence of the specific sulfate position on the subsequent binding and release of growth factors was investigated. For this purpose, the hydrogel platform was extended to include SH, N-DSH, 6O-DSH, 2O-DSH, 6O+N-DSH and cDSH (see **Figure 12**).[155] VEGF release was unaffected by 2O-DSH HEP, whereas the removal of the other sulfate groups caused a stepwise increase in VEGF release. Hydrogels formed from cDSH exhibited ~90% VEGF release but anticoagulant activity of less than 1%. These results were independent of the type of desulfation method (Figure 12). Thus, all the applied desulfation protocols blocked HEP anticoagulant activity, i.e., effectively prevented bleeding. *In vitro* studies showed a pronounced pro-angiogenic response of HUVECs, as indicated by enhanced cell migration and tube formation, which was dependent on the VEGF amounts released from hydrogels containing selectively desulfated HEP (Figure 12).

Desulfated HEP hydrogels with low anticoagulant activity were transplanted into db/db mice to investigate the effects of modulating VEGF release from the matrices. Hydrogels with low sulfate content (11% of the initial HEP) were found to be superior in terms of efficacy of VEGF administration, low anticoagulant activity and promotion of angiogenesis *in vivo* (Figure 12).

In an independent approach, Temenoff and co-workers used a thiolated N-DSH crosslinked with PEGDA to form hydrogels for the sustained release of SDF-1α.[156] The SDF-1α-releasing matrices stimulated the migration of bone marrow cells *in vitro* and the spatially localized recruitment of anti-inflammatory monocytes in a dorsal skinfold window chamber in mice.

4.3 Cell-Responsive Release

Interactive materials that are capable of responding to varying environmental conditions through varied characteristics are instrumental for customized exogenous cell-fate control in tissue engineering and offer exciting new options in drug delivery. The enzymatic cleavage of hydrogel materials for the localized modulation of growth factor release and the growth factor-dependent degradation of hydrogels both represent well-elaborated examples of related approaches. Furthermore, a recently introduced material demonstrates how the release of bioactives can be adjusted in a feedback loop, enabling the homeostatic control of complex biochemical reactions in living tissues, such as blood coagulation activation.

4.3.1 MMP-Degradable GAG Hydrogels—Like the PEG-based MMP-degradable hydrogels pioneered by Lutolf and Hubbell,[157] GAG-containing hydrogels can be made susceptible to degradation by cell-secreted proteases through the incorporation of matrix metalloprotease (MMP)-cleavable peptide crosslinkers. MMP peptide motifs are typically incorporated into GAG-based hydrogels via a Michael-type addition between thiols from cysteine residues of the peptides and reactive end groups (e.g., acrylates and maleimides) from the macromers, allowing the embedding of cells and molecules during gelation. The cell-mediated degradation of GAG-based hydrogels permits the tunable release of the encapsulated bioactive factors via cellular cues and supports cellular morphogenesis into a variety of tissue structures, resulting in matrix remodeling and tissue regeneration.

A cell-responsive PEG-HEP hydrogel including an MMP-cleavable peptide (see section 3.1.1)[18,19] was successfully used for the delivery of chemokines such as VEGF and SDF-1α, and the release of growth factors was significantly accelerated in the presence of collagenase IV. The cell-mediated release of growth factors from these hydrogels resulted in a strong pro-angiogenic response both *in vitro* and *in vivo*, demonstrating the potential of these materials to support cardiovascular tissue engineering.[21,135]

More recently, the in situ formation of MMP-degradable PEG-HEP hydrogels based on a Michael-type addition between maleimide-functionalized HEP and thiol-containing PEG-MMP peptide conjugates was reported (**Figure 13**).[28,158] The rapid gelation of these materials allowed the facile in situ encapsulation of soluble growth factors and cells. The cell-mediated degradation and subsequent VEGF delivery exhibited a significant effect on cell spreading and endothelial cell morphogenesis.[28] These bioresponsive hydrogels were subsequently used for the sustained release of multiple pro-angiogenic growth factors (VEGF, FGF-2 and SDF-1α) to enhance the formation of endothelial capillary networks and to construct 3D tumor vascularization models, providing significant insights into the development of therapeutic strategies against angiogenesis-dependent tumors.[158] The underlying concept was based on a well-adjusted co-culture system of MSCs and HUVECs within a triple-factor (VEGF, FGF-2 and SDF-1α)-functionalized, RGD-modified, MMP-degradable, soft (~200 Pa) starPEG-HEP hydrogel matrix. This system was able to maintain a mature capillary network for more than four weeks *in vitro*, thus opening new possibilities for advanced *in vitro* organoid models.

In an extension of that work, triple cultures of HUVECs, MSCs and various breast (MCF-7 and MDA-MB-231) and prostate cancer cell types (LNCaP and PC3) were cultivated to establish relevant vascularized 3D cancer models *in vitro*.[159] This systematic study using different chemotherapeutic drugs and angiogenic inhibitors compared conventional 2D, 3D tumor-only and triple-culture models. Interestingly, it was found that the dose required to stop the proliferation of cancer cells was much higher in 3D than in artificial 2D culture - a finding that is consistent with similar findings *in vivo* and thus demonstrates the relevance of the concept established here. Accordingly, multifunctional, multifactorial starPEG-HEP hydrogels appear to be highly promising candidates for advanced organ culture models and thus may be utilized to minimize expensive and ethically problematic animal experiments.[160]

Likewise, Segura and co-workers developed a series of proteolytically degradable HA hydrogels based on the Michael-type addition of acrylamide-functionalized HA and bis-cysteine-containing MMP peptide crosslinkers.[161] These MMP-degradable HA hydrogels were exploited to guide stem cell differentiation *in vitro* and to promote tissue repair in diabetic wounds and in the brain after stroke through the delivery of stem cells or nanoparticles containing bioactive signals. Integrin-binding peptide concentration and presentation were exploited to modulate neuroprogenitor stem cell (iPS-NPC) and MSC differentiation. The relative concentrations of IKVAV, YIGSR, and RGD were optimized through the multifactorial design of experiments (DOE) to arrive at concentrations that enhanced stem cell survival and improved differentiation toward neurons.[162] In a separate study, RGD presentation was modulated from homogeneous to clustered and was shown to

modulate integrin and stem cell marker expression.[163] The same hydrogel materials have been used *in vivo* as a dual scaffold and transplantation vehicle for iPS-NPCs or as a scaffold and bioactive signal delivery vehicle to promote tissue repair. The transplantation of iPS-NPCs from MMP-HA hydrogels resulted in enhanced differentiation of the transplanted cells.[164]

The incorporation of growth factors into hydrogel scaffolds is a general approach to guiding the fate of encapsulated or infiltrating cells. However, the direct encapsulation of growth factors during Michael-type addition hydrogel formation suffers from reduced growth factor activity through disulfide exchange reactions (in the case of thiol-containing crosslinkers) and limited control over the release kinetics of the growth factors. The Segura laboratory has pioneered the use of protein core nanocapsules to deliver growth factors.[165,166] Nanocapsules are formed through the in situ radical polymerization of acrylate- and acrylamide-containing monomers and peptide crosslinkers around a protein core. The result is a protein surrounded by a protease-degradable hydrated polymeric shell. By changing the enantiomer of the amino acids in the peptide crosslinker from L to D, the kinetics of enzymatic cleavage were modulated to generate the sustained or sequential delivery of one or several growth factors. Compared to direct growth factor encapsulation, the encapsulation of growth factor nanocapsules within HA-MMP hydrogels resulted in decreased disulfide exchange reactions, which increased the activity of the encapsulated protein[166] and the controlled release of the growth factor *in vitro* and *in vivo*.[165] Upon the implantation of VEGF nanocapsule-loaded hydrogels, enhanced vascularization of the brain after stroke (see **Figure 14**)[165] and enhanced skin wound healing were observed.[167] The Segura laboratory has also made considerable efforts to deliver plasmid DNA from MMP-degradable HA hydrogels.[168] Utilizing a cage nanoparticle encapsulation approach to prevent DNA/PEI polyplex aggregation during hydrogel gelation,[169] they were able to deliver DNA plasmids encoding human VEGF165 (pro-angiogenic factor) and mammalian GFP-firefly luciferase (reporter) to enhance the angiogenic response and diabetic wound healing.

Burdick and co-workers developed injectable and MMP-sensitive HA-based hydrogels that locally release a recombinant tissue inhibitor of MMPs (rTIMP-3) in response to MMP activity (**Figure 15**).[170] The hydrogels were formed rapidly by a condensation reaction between aldehyde (ALD) and hydrazine (HYD) groups in a three-macromer system that included HA-ALD, dextran sulfate-ALD and HA-peptide-HYD. The incorporation of dextran sulfate and an MMP-cleavable peptide into the hydrogels allowed the sequestration of rTIMP-3 and on-demand MMP inhibition via MMP-mediated degradation. The targeted delivery of the hydrogel/rTIMP-3 construct to regions of MMP overexpression following myocardial infarction significantly reduced MMP activity and attenuated adverse left ventricular remodeling in a porcine model of myocardial infarction. This strategy provides a vivid example of the design of bioresponsive hydrogels whose properties can change in response to a specific set of biological stimuli.

In addition to MMP-sensitive GAG hydrogels, Kiick and co-workers developed cell surface receptor-responsive HEP hydrogels directly using growth factors as crosslinks (**Figure 16**).[171] These non-covalently associated hydrogel networks were produced via an interaction between low-molecular-weight HEP-modified star polymers (PEG-LMWHEP)

and the dimeric, HEP-binding growth factor VEGF. Taking advantage of the receptor-mediated targeting of VEGF to VEGFR-2 receptors, the hydrogels demonstrated receptor-mediated gel erosion and the VEGFR-2-responsive sustained release of VEGF.[171a] The selective erosion and cell-responsive release of VEGF from these hydrogels was further studied using VEGFR-2-overexpressing PAE/KDR cells (porcine aortic endothelial cells equipped with the transcript for the kinase insert domain receptor).[171b] The receptor-responsiveness of the hydrogel and the cell-mediated release of VEGF were evidenced by the observation that the 100% release of VEGF and complete hydrogel erosion occurred exclusively in the presence of PAE/KDR as well as by the increased proliferation of VEGFR-2-expressing cells. These novel studies demonstrate a robust approach for the targeted delivery of receptor-binding bioactive molecules in numerous therapeutic applications.

4.4 Autoregulative Release

Extending the above-discussed concept of bioresponsive polymer architectures can allow the feedback-controlled regulation of the release of bioactives, a principle that even more closely resembles the homeostatic adaptation of living tissues. Using the anticoagulant activity of the GAG HEP, the regulation of blood coagulation through the interplay of enzyme-mediated activation and inhibition processes was examined as an example of this approach to a new type of interactive material. HEP inactivates thrombin, the key enzyme in the blood coagulation cascade,[172] and is commonly used in the application of medical devices to inhibit the activation of blood coagulation. Hydrogels made of starPEG and HEP crosslinked by a thrombin-sensitive peptide linker were used to establish a thrombin-responsive, adaptive HEP release system.[173] In this system, if blood coagulation is activated, (A) thrombin is formed from prothrombin and initiates the self-amplifying blood coagulation cascade while simultaneously (B) cleaving the hydrogel, resulting in the release of HEP followed by (C) the HEP-catalyzed formation of the thrombin-antithrombin complex, which in turn inactivates thrombin and (D) terminates the degradation of the hydrogel (see **Figure 17**).

Thrombin-cleavable HEP hydrogels were experimentally shown to release HEP in a manner that was dependent on the thrombin concentration and the degree of crosslinking, i.e., the HEP release was strictly correlated with the trigger concentration and was further tunable through the network characteristics. The performance of the HEP-releasing hydrogels was tested in a human whole-blood incubation assay. As expected, the anticoagulant effect was directly correlated with the released HEP and the crosslinking degree of the hydrogels, whereas a hydrogel crosslinked with a scrambled peptide sequence showed significantly lower anticoagulant activity. In an extended feasibility test without the addition of any soluble anticoagulant, using ePTFE and HEP-end-grafted ePTFE as clinically applied reference materials, non-cleavable and thrombin-cleavable hydrogels were compared in a repeated (1 h + 1 h) incubation cycle. Blood in contact with the thrombin-responsive hydrogel did not show any clotting effects, whereas all the compared materials resulted in massive coagulation. This system is clearly a promising means of coating medical devices to avoid systemic overdosage of HEP and provide long-term protection against coagulation. The exemplified concept for interactive materials can be considered a new paradigm for the

feedback-controlled administration of drugs and bioactives along various therapeutic avenues and may even pave the way for autonomous functional compartments in synthetic biology.

5. Perspective

A number of current developments can be expected to further extend the options involving GAG-based functional materials in the future. Namely, the availability of tailor-made, widely tunable GAG motifs and advanced methodologies for the design and experimental screening of GAG-based functional materials will create exciting new opportunities. Relying on a key feature of GAGs, their capability to complex a broad variety of cytokines, a new field of applications for cytokine-scavenging biomaterials is envisioned on the horizon.

5.1 Synthetic and Recombinant GAGs

All clinically applied GAGs, such as the widely used anticoagulant HEP, are currently isolated from animal sources. The resulting batch-to-batch variations and even serious quality issues—including the contamination of HEP with oversulfated CS, which caused approximately 100 deaths in the US in 2008[174] —limit the applications of GAGs in medicine, biotechnology and tissue engineering. Accordingly, the development of synthetic routes to create well-defined GAG building blocks for biomedical applications has attracted increasing interest during recent years.

Pioneered by Seeberger and co-workers, automated solid-phase oligosaccharide synthesis has become available, addressing the need for functional disaccharide precursors to form oligosaccharides with well-defined structure and conformation.[175] The ongoing efforts of the Seeberger group are directed toward the automated solid-phase synthesis of larger building blocks, such as CS-GAGs[176] or DS oligosaccharides,[177] which will become scalable.[178] Progress in carbohydrate sequencing and high-throughput screening based on carbohydrate arrays can be expected to pave the way for novel combinatorial approaches[175a] to GAG-based material development, enabling advanced diagnostics and therapeutic applications.

As an alternative, the preparation of sulfated, GAG-mimicking polymers via the backbone modification of polysaccharides does not require sophisticated and complex solid-phase methods starting from disaccharide building blocks. Several well-established protocols for the chemical sulfation of chitosan, cellulose, starch, alginate and HA, as reviewed in,[179] extend the range of customized GAG-analogous polymers. Langer and co-workers designed a selectively C6-OH-sulfated HA that could be used for the separation/selective binding of the angiogenic and anti-angiogenic isoforms of VEGF165 for applications in anti-angiogenic therapies.[180] In a similar approach, Hofbauer and co-workers utilized selectively sulfated HA and modified CS to analyze the impact of GAG sulfation on Wnt signaling and bone homeostasis.[181] However, GAG-mimicking polymers based on other biopolymers cannot overcome the disadvantages mentioned above, i.e., product heterogeneity and possible immunogenic effects persist.[179]

In addition to backbone modification, chemical and chemoenzymatic protocols have been developed to utilize enzymes for the synthesis or modification of GAGs.[182] Different routes either start from GAG backbone polymers extracted from any organism followed by subsequent *in vitro* modification, the cleaving of GAG chains with degradation enzymes and subsequent modifications *in vitro,* or the classical bottom-up formation of GAG chains with synthases/GTases from uridine diphosphate sugars *in vitro*.[2] The latter concept is advantageous because it produces well-defined GAG structures, but it is restricted by the currently limited availability of uridine diphosphate sugars.[179] Linhardt and co-workers established the synthesis of ultra-low-molecular-weight HEP starting from a simple disaccharide unit that shows excellent anticoagulant activity and good pharmacokinetic properties and is scalable for use as a building block for biomaterials.[183] Based on this synthetic route, well-defined HS block copolymers were synthesized and utilized to study FGF-2 signaling in murine immortalized bone marrow (BaF3) cells in a microtiter array.[184]

Well-defined GAG building blocks can also be obtained by dedicated expression techniques. In nature, GAGs are synthesized in the Golgi apparatus of most animal cells on the surface of a protein core (with the exception of the non-sulfated HA, which is synthesized without protein conjugation), forming proteoglycans, a major component of the ECM. HS/HEP proteoglycans, including perlecan, agrin, syndecans and glypicans, have been recombinantly expressed in mammalian cells, such as Chinese hamster ovary (CHO) and human embryonic kidney cells (HEK-293 and HEK-293T).[179] Further optimization is needed to precisely control the GAG chain length and the specific sulfation pattern, as the differences currently found in the structure and length of the expressed GAGs may be attributed to different residence times of the protein core in the Golgi or to missing post-translational modifications.[185] The metabolic engineering of Golgi-lacking cells, such as *E. coli*, is considered even more difficult but is being targeted by dedicated ongoing studies. For a recent review of the expression techniques currently used for the formation of GAGs, the reader is referred to Suflita et al.[186]

Of note, control of the size and charge pattern in well-defined synthetic GAGs extends the possibilities of regulating the conformation and hydration of GAG building blocks, generating materials with tailored physical characteristics and adjustable transport and binding properties for soluble signaling molecules.

5.2 Rational and Combinatorial Material Design

Adjustment of the physical network properties and biomolecular functionalization of GAG-based materials—as required to systematically unravel the roles of exogenous cues in cell-fate control—was successfully implemented using a rational design strategy for defined polymer networks with varying mechanical properties but constant biomolecular composition.[134] A mean field approach was applied to identify conditions in which the balance of elastic, electrostatic/osmotic, and excluded volume forces resulted in a constant HEP volume density within starPEG-HEP hydrogels with gradually varied network properties (see **Figure 18**A and B). Using this approach, the mechanical properties (storage moduli) of the biohybrid hydrogel could be varied over a broad range, from ~1 kPa to ~15 kPa, at an invariant HEP concentration (see Figure 18B). As discussed in sections 2 and 4,

secondary functionalization schemes with cell-adhesive peptides (e.g., RGD) and HEP-affine soluble signaling molecules (e.g., VEGF) by covalent and non-covalent conjugation to HEP also allow the decoupling of related signaling characteristics from the mechanical network properties. The mean field approach was recently extended to explore the swelling and storage moduli of hydrogels formed from selectively desulfated HEP derivatives[154] to customize the release of growth factors from similarly defined hydrogel networks. It is envisioned that the established theory-driven design of biohybrid polymer networks can offer a powerful, general option for tailoring multifunctional GAG-based materials to become instrumental in biotechnology, medicine and further fields.

Regarding the recent progress in combinatorial approaches to bioactive PEG-based materials achieved in the pioneering studies of Lutolf et al.,[187] high-throughput approaches for the identification of effective combinations of multiple matrix-associated, cell-instructive signals can be adapted for use with GAG-PEG matrix platforms. For example, PEG-GAG hydrogel arrays may offer a simple and highly effective means of screening non-covalently conjugated cytokines. Furthermore, the defined microfluidic administration of multiple soluble cues through hydrogel matrices can be enhanced through the implementation of factor-binding GAG components that act as sources or sinks for growth factors, delaying and directing diffusive transport across the matrices.

The biomolecular and mechanical signals presented by the ECM are spatially and temporally resolved, although existing macroscale methodologies to produce cell-instructive biomaterial matrices remain limited with respect to the modulation of important biological processes such as tissue regeneration or tumor metastasis.[13,92,188] The development of materials with spatiotemporally customized biomolecular and physical cell signaling characteristics defines an obvious but heretofore unmet need for a new generation of biomaterials.[5,187d] Hydrogel-based approaches employing GAGs will have continued importance in this regard, particularly for growth factor delivery, as the complex processes of cell migration, differentiation and proliferation typically require the presence of multiple growth factors and their spatiotemporal distribution at distinct stages.[189] Although GAG-based hydrogels have been employed for the parallel release of multiple growth factors, studies have shown that the sequential delivery of multiple growth factors would better mimic the temporal profile of the natural healing process.[190] Motivated by recent advances in hierarchically structured, multicomponent hydrogels and orthogonal degradation chemistries, GAG-based hydrogels with sequential release characteristics could be designed by incorporating a secondary nanoparticle domain (e.g., liposomes or PLGA nanoparticles)[191] into a GAG-based network and introducing multiple degradable linkages (e.g., wavelength-selective photocleavable units)[192] into the precursors. Combined with the inherent biological activities of GAGs, such GAG-based materials could provide physiologically relevant release profiles and spatial gradients of multiple growth factors, with the potential to improve tissue regeneration.

In addition to opportunities to chemically control the degradation and delivery profiles of bulk GAG-based hydrogel matrices, novel manufacturing approaches that combine the nanoplotting of GAG-based hydrogels and microfluidic techniques to enable the fabrication of miniaturized hydrogel-based 3D culture arrays would also afford exciting opportunities

for precise control over local growth factor concentrations and orthogonally graded mechanical properties (see **Figure 19**). Utilizing such hydrogel arrays should enable simultaneous high-throughput exploration of the influences of mechanical and morphogen gradients on cells embedded in 3D arrays.

5.3 Cytokine-Scavenging Materials

The unique capability of sulfated GAGs to form complexes with proteins (see section 4.2) suggests that matrices with a high content of sulfated GAGs may provide an effective means for the localized scavenging of cytokines *in vivo*. This possibility offers promising new biomaterial features, e.g., the scavenging and effective removal of pro-inflammatory cytokines in biomaterial-aided wound healing. Referring to the recent review by Murphy et al.[193] of parameters that govern the natural mechanisms of growth factor sequestering by ECMs and of bioengineering approaches that use similar principles to modulate cell function, we hypothesize that GAG-PEG matrices incorporating GAGs with tailored structure, size, sulfation pattern and distribution can complement the currently applied principles for growth factor administration both in cell culture and *in vivo*. Along these lines, the application of unloaded GAG-based hydrogels may be used to redirect the growth factor gradients that govern tissue formation and regeneration *in vivo*.

Acknowledgements

This work was supported by the Deutsche Forschungsgemeinschaft through CRC TR 67 (UF, CW), CRC SFB 655 (CW), FR 3367/2-1 (UF), WE 2539-7 (CW), and FOR/EXC999 (CW), by the Leibniz Association through SAW-2011-IPF-2 68 (CW), by the European Union through the FP7 projects ANGIOSCAFF (grant agreement no. 214402-2, CW) and HydroZONES (grant agreement no. 309962, CW) and through the Federal Ministry of Education and Research of Germany through the initiative “Unternehmen Region Zwanzig20” project RESPONSE (FKZ 03ZZ0903E, CW) and initiative “Innovative Gesundheitstechnologien” project EXASENS (FKZ 13N13859, CW).

Biography

Uwe Freudenberg is the group leader for Matrix Engineering at the Institute of Biofunctional Polymer Materials at the Leibniz Institute for Polymer Research Dresden, Germany (IPF). He received his PhD (Dr.-Ing.) at the Technische Universität Dresden in Material Science in 2007. His current research focuses on the design and application of multifunctional polymer materials for biomedical applications with special emphasis on the independent modulation of physical and biomolecular network properties resulting in more than 45 papers and patents in the area.

Yingkai Liang is currently a Ph.D. candidate in Materials Science and Engineering at the University of Delaware. He received his bachelor degree in Polymer Science and Engineering from Sun Yat-sen University in China in 2011, and subsequently began his doctoral research at the University of Delaware under the supervision of Professor Kristi Kiick. His current research is focused on developing polymeric hydrogels for controlled drug delivery applications.

References

1. Häcker U, Nybakken K, Perrimon N. Nat. Rev. Mol. Cell. Biol. 2005; 6:530. [PubMed: 16072037]
2. DeAngelis PL, Liu J, Linhardt RJ. Glycobiology. 2013; 23:764. [PubMed: 23481097]
3. Mouw JK, Ou G, Weaver VM. Nat. Rev. Mol. Cell. Biol. 2014; 15:771. [PubMed: 25370693]
4. a Capila I, Linhardt RJ. Angew. Chem. Int. Edit. 2002; 41:391.b Garg, HG.; Linhardt, RJ.; Hales, CA. Chemistry and Biology of Heparin and Heparan Sulfate. Elsevier; Oxford, United Kingdom: 2011.
5. Yan D, Lin X. Cold Spring Harbor Perspectives in Biology. 2009; 1:a002493. [PubMed: 20066107]
6. Yu SR, Burkhardt M, Nowak M, Ries J, Petrasek Z, Scholpp S, Schwille P, Brand M. Nature. 2009; 461:533. [PubMed: 19741606]
7. a Gurdon JB, Bourillot PY. Nature. 2001; 413:797. [PubMed: 11677596] b Rogers KW, Schier AF. Annu. Rev. Cell Dev. Biol. 2011; 27:377. [PubMed: 21801015]
8. a Lau LW, Cua R, Keough MB, Haylock-Jacobs S, Yong VW. Nat. Rev. NeuroSci. 2013; 14:722. [PubMed: 23985834] b Bishop JR, Schuksz M, Esko JD. Nature. 2007; 446:1030. [PubMed: 17460664]
9. a Parish CR. Nat. Rev. Immunol. 2006; 6:633. [PubMed: 16917509] b Taylor KR. FASEB J. 2006; 20:9. [PubMed: 16394262]
10. a Sasisekharan R, Shriver Z, Venkataraman G, Narayanasami U. Nat. Rev. Cancer. 2002; 2:521. [PubMed: 12094238] b Afratis N, Gialeli C, Nikitovic D, Tsegenidis T, Karousou E, Theocharis AD, Pavão MS, Tzanakakis GN, Karamanos NK. FEBS J. 2012; 279:1177. [PubMed: 22333131] c Belting M. Thromb. Res. 2014; 133:95.
11. Scott RA, Panitch A. Wiley Interdiscip. Rev. Nanomed. Nanobiotechnol. 2013; 5:388. [PubMed: 23606640]
12. Yannas IV, Tzeranis DS, Harley BA, So PTC. Phil. Trans. R. Soc. A. 2010; 368:2123. [PubMed: 20308118]
13. Discher DE, Mooney DJ, Zandstra PW. Science. 2009; 324:1673. [PubMed: 19556500]
14. a Lutolf MP, Gilbert PM, Blau HM. Nature. 2009; 462:433. [PubMed: 19940913] b Lutolf MP, Hubbell JA. Nat. Biotechnol. 2005; 23:47. [PubMed: 15637621]
15. Ravanti L, Kähäri VM. Int. J. Mol. Med. 2000; 6:391. [PubMed: 10998429]
16. Freudenberg U, Hermann A, Welzel PB, Stirl K, Schwarz SC, Grimmer M, Zieris A, Panyanuwat W, Zschoche S, Meinhold D, Storch A, Werner C. Biomaterials. 2009; 30:5049. [PubMed: 19560816]
17. Nagase H, Fields GB. Biopolymers. 1996; 40:399. [PubMed: 8765610]
18. Tsurkan MV, Levental KR, Freudenberg U, Werner C. Chem. Commun. 2010; 46:1141.

19. Tsurkan MV, Chwalek K, Levental KR, Freudenberg U, Werner C. Macromol. Rapid Commun. 2010; 31:1529. [PubMed: 21567562]
20. Novosel EC, Kleinhans C, Kluger PJ. Adv. Drug Deliv. Rev. 2011; 63:300. [PubMed: 21396416]
21. Chwalek K, Levental KR, Tsurkan MV, Zieris A, Freudenberg U, Werner C. Biomaterials. 2011; 32:9649. [PubMed: 21937106]
22. Tsurkan MV, Chwalek K, Schoder M, Freudenberg U, Werner C. Bioconjug. Chem. 2014; 25:1942. [PubMed: 25297697]
23. a Hirano Y, Okuno M, Hayashi T, Goto K, Nakajima A. J. Biomater. Sci. Polym. Ed. 1993; 4:235. [PubMed: 8476793] b Pierschbacher MD, Ruoslahti E. J. Biol. Chem. 1987; 262:17294. [PubMed: 3693352]
24. Trappmann B, Gautrot JE, Connelly JT, Strange DGT, Li Y, Oyen ML, Cohen Stuart MA, Boehm H, Li B, Vogel V, Spatz JP, Watt FM, Huck WTS. Nat. Mater. 2012; 11:642. [PubMed: 22635042]
25. a Pampaloni F, Reynaud EG, Stelzer E. Nat. Rev. Mol. Cell Bio. 2007; 8:839. [PubMed: 17684528] b Tibbitt MW, Anseth KS. Biotechn. Bioeng. 2009; 103:655.
26. Van Tomme SR, Storm G, Hennink WE. Int. J. Pharm. 2008; 355:1. [PubMed: 18343058]
27. Phelps EA, Enemchukwu NO, Fiore VF, Sy JC, Murthy N, Sulchek TA, Barker TH, García AJ. Adv. Mater. 2012; 24:64. [PubMed: 22174081]
28. Tsurkan MV, Chwalek K, Prokoph S, Zieris A, Levental KR, Freudenberg U, Werner C. Adv. Mater. 2013; 25:2606. [PubMed: 23576312]
29. Kim J, Park Y, Tae G, Lee KB, Hwang SJ, Kim IS, Noh I, Sun K. J. Mater. Sci.-Mater. Med. 2008; 19:3311. [PubMed: 18496734]
30. Nie T, Akins RE, Kiick KL. Acta Biomater. 2009; 5:865. [PubMed: 19167277]
31. Benoit DSW, Durney AR, Anseth KS. Biomaterials. 2007; 28:66. [PubMed: 16963119]
32. Benoit DSW, Collins SD, Anseth KS. Adv. Funct. Mater. 2007; 17:2085. [PubMed: 18688288]
33. Wieduwild R, Tsurkan M, Chwalek K, Murawala P, Nowak M, Freudenberg U, Neinhuis C, Werner C, Zhang Y. J. Am. Chem. Soc. 2013; 135:2919. [PubMed: 23388040]
34. Wieduwild R, Krishnan S, Chwalek K, Boden A, Nowak M, Drechsel D, Werner C, Zhang Y. Angew. Chem. Int. Edit. 2015; 54:3962.
35. Tan H, Zhou Q, Qi H, Zhu D, Ma X, Xiong D. Macromol. Biosci. 2012; 12:621. [PubMed: 22454284]
36. Kharkar PM, Kiick KL, Kloxin AM. Chem. Soc. Rev. 2013; 42:7335. [PubMed: 23609001]
37. Burdick JA, Murphy WL. Nat. Commun. 2012; 3:1269. [PubMed: 23232399]
38. a Burdick JA, Prestwich GD. Adv. Mater. 2011; 23:H41. [PubMed: 21394792] b Miller T, Goude MC, McDevitt TC, Temenoff JS. Acta Biomater. 2014; 10:1705. [PubMed: 24121191]
39. a Xu X, Jha AK, Harrington DA, Farach-Carson MC, Jia X. Soft Matter. 2012; 8:3280. [PubMed: 22419946] b Dicker KT, Gurski LA, Pradhan-Bhatt S, Witt RL, Farach-Carson MC, Jia X. Acta Biomaterialia. 2014; 10:1558. [PubMed: 24361428]
40. Takahashi A, Suzuki Y, Suhara T, Omichi K, Shimizu A, Hasegawa K, Kokudo N, Ohta S, Ito T. Biomacromolecules. 2013; 14:3581. [PubMed: 24004342]
41. Patterson J, Siew R, Herring SW, Lin ASP, Guldberg R, Stayton PS. Biomaterials. 2010; 31:6772. [PubMed: 20573393]
42. a Pitarresi G, Pierro P, Palumbo FS, Tripodo G, Giammona G. Biomacromolecules. 2006; 7:1302. [PubMed: 16602753] b Palumbo FS, Pitarresi G, Fiorica C, Matricardi P, Albanese A, Giammona G. Soft Matter. 2012; 8:4918.
43. Kim IL, Mauck RL, Burdick JA. Biomaterials. 2011; 32:8771. [PubMed: 21903262]
44. Sahoo S, Chung C, Khetan S, Burdick JA. Biomacromolecules. 2008; 9:1088. [PubMed: 18324776]
45. Chung C, Beecham M, Mauck RL, Burdick JA. Biomaterials. 2009; 30:4287. [PubMed: 19464053]
46. Traverso N, Ricciarelli R, Nitti M, Marengo B, Furfaro AL, Pronzato MA, Marinari UM, Domenicotti C. Oxid. Med. Cell. Longev. 2013; 2013:972913. [PubMed: 23766865]
47. a Singh S, Topuz F, Hahn K, Albrecht K, Groll J. Angew. Chem. Int. Edit. 2013; 52:3000.b Ejaz M, Yu H, Yan Y, Blake DA, Ayyala RS, Grayson SM. Polymer. 2011; 52:5262.c Wu ZM, Zhang XG,

Zheng C, Li CX, Zhang SM, Dong RN, Yu DM. Eur. J. Pharm. Sci. 2009; 37:198. [PubMed: 19491006]

48. a Shu XZ, Liu Y, Luo Y, Roberts MC, Prestwich GD. Biomacromolecules. 2002; 3:1304. [PubMed: 12425669] b Shu XZ, Liu Y, Palumbo F, Prestwich GD. Biomaterials. 2003; 24:3825. [PubMed: 12818555]
49. Zhang J, Skardal A, Prestwich GD. Biomaterials. 2008; 29:4521. [PubMed: 18768219]
50. Choh S-Y, Cross D, Wang C. Biomacromolecules. 2011; 12:1126. [PubMed: 21384907]
51. Ossipov D, Kootala S, Yi Z, Yang X, Hilborn J. Macromolecules. 2013; 46:4105.
52. Baldwin AD, Kiick KL. Polym. Chem. 2013; 4:133. [PubMed: 23766781]
53. Baldwin AD, Kiick KL. Bioconjug. Chem. 2011; 22:1946. [PubMed: 21863904]
54. Liang Y, Kiick KL. Polym. Chem. 2014; 5:1728.
55. a Kloxin AM, Kasko AM, Salinas CN, Anseth KS. Science. 2009; 324:59. [PubMed: 19342581] b Deforest CA, Anseth KS. Nature Chem. 2011; 3:925. [PubMed: 22109271]
56. a Griffin DR, Schlosser JL, Lam SF, Nguyen TH, Maynard HD, Kasko AM. Biomacromolecules. 2013; 14:1199. [PubMed: 23506440] b Griffin DR, Kasko AM. ACS Macro Lett. 2012; 1:1330. [PubMed: 25285242] c Kharkar PM, Kiick KL, Kloxin AM. Polym. Chem. 2015; 6:5565. [PubMed: 26284125]
57. a Zhao H, Sterner ES, Coughlin EB, Theato P. Macromolecules. 2012; 45:1723.b Bao C, Zhu L, Lin Q, Tian H. Adv. Mater. 2015; 27:1647. [PubMed: 25655424]
58. Tsurkan MV, Wetzel R, Pérez-Hernández HR, Chwalek K, Kozlova A, Freudenberg U, Kempermann G, Zhang Y, Lasagni AF, Werner C. Adv. Healthc. Mater. 2015; 4:516. [PubMed: 25323149]
59. You J, Haque A, Shin DS, Son KJ, Siltanen C, Revzin A. Adv. Funct. Mater. 2015; 25:4650.
60. a Li Q, Williams CG, Sun DDN, Wang J, Leong K, Elisseeff JH. J. Biomed. Mater. Res. A. 2004; 68:28. [PubMed: 14661246] b Nie T, Baldwin A, Yamaguchi N, Kiick KL. J. Control. Release. 2007; 122:287. [PubMed: 17582636]
61. Welzel PB, Prokoph S, Zieris A, Grimmer M, Zschoche S, Freudenberg U, Werner C. Polymers. 2011; 3:602.
62. Annabi N, Nichol JW, Zhong X, Ji C, Koshy S, Khademhosseini A, Dehghani F. Tissue Eng. Part B. Rev. 2010; 16:371. [PubMed: 20121414]
63. Welzel PB, Grimmer M, Renneberg C, Naujox L, Zschoche S, Freudenberg U, Werner C. Biomacromolecules. 2012; 13:2349. [PubMed: 22758219]
64. Welzel PB, Friedrichs J, Grimmer M, Vogler S, Freudenberg U, Werner C. Adv. Healthc. Mater. 2014; 3:1849. [PubMed: 24729299]
65. Fratzl, P. Collagen: Structure and Mechanics. Springer; New York, USA: 2008.
66. Joly P, Duda GN, Schöne M, Welzel PB, Freudenberg U, Werner C, Petersen A. PLoS One. 2013; 8:e73545. [PubMed: 24039979]
67. Newland B, Welzel PB, Newland H, Renneberg C, Kolar P, Tsurkan M, Rosser A, Freudenberg U, Werner C. Small. 2015; 11:5047. [PubMed: 26237446]
68. Newland B, Newland H, Werner C, Rosser A, Wang W. Prog. Polym. Sci. 2015; 44:79.
69. Cascone MG, Lazzeri L, Sparvoli E, Scatena M, Serino LP, Danti S. J. Mater. Sci.-Mater. Med. 2004; 15:1309. [PubMed: 15747183]
70. Lee KY, Jeong L, Kang YO, Lee SJ, Park WH. Adv. Drug Deliv. Rev. 2009; 61:1020. [PubMed: 19643155]
71. Um IC, Fang D, Hsiao BS, Akio Okamoto A, Chu B. Biomacromolecules. 2004; 5:1428. [PubMed: 15244461]
72. Li J, He A, Han CC, Fang D, Hsiao BS, Chu B. Macromol. Rapid Commun. 2006; 27:114.
73. Sokolov JC, Prestwich GD, Clark R, Rafailovich MH. Biomaterials. 2006; 27:3782. [PubMed: 16556462]
74. Ji Y, Ghosh K, Li B, Sokolov JC. Macromol. Sci. 2006; 6:811.
75. Viswanathan G, Murugesan S, Pushparaj V, Nalamasu O, Ajayan PM, Linhardt RJ. Biomacromolecules. 2006; 7:415. [PubMed: 16471910]

76. Luong-Van E, Grøndahl L, Chua KN, Leong KW, Nurcombe V, Cool SM. Biomaterials. 2006; 27:2042. [PubMed: 16305806]
77. Patel S, Kurpinski K, Quigley R, Gao H, Hsiao B, Mu-Ming Poo A, Li Song. Nano Lett. 2007; 7:2122. [PubMed: 17567179]
78. a Thoniyot P, Tan MJ, Karim AA, Young DJ, Loh XJ. Adv. Sci. 2015; 2:1400010.b Merino S, Martín C, Kostarelos K, Prato M, Vázquez E. ACS Nano. 2015; 9:4686. [PubMed: 25938172]
79. Gaharwar AK, Peppas NA, Khademhosseini A. Biotechnol. Bioeng. 2014; 111:441. [PubMed: 24264728]
80. Hall-Stoodley L, Costerton JW, Stoodley P. Nat. Rev. Micro. 2004; 2:95.
81. Fischer M, Vahdatzadeh M, Konradi R, Friedrichs J, Maitz MF, Freudenberg U, Werner C. Biomaterials. 2015; 56:198. [PubMed: 25934292]
82. Zhang Y, Sun Y, Yang X, Hilborn J, Heerschap A, Ossipov DA. Macromol. Biosci. 2014; 14:1249. [PubMed: 24863175]
83. a García-Astrain C, Chen C, Burón M, Palomares T, Eceiza A, Fruk L, Corcuera MÁ, Gabilondo N. Biomacromolecules. 2015; 16:1301. [PubMed: 25785360] b García-Astrain C, Ahmed I, Kendziora D, Guaresti O, Eceiza A, Fruk L, Corcuera MA, Gabilondo N. RSC Adv. 2015; 5:50268.
84. Skardal A, Zhang J, McCoard L, Oottamasathien S. Adv. Mater. 2010; 22:4736. [PubMed: 20730818]
85. a Larson N, Ghandehari H. Chem. Mater. 2012; 24:840. [PubMed: 22707853] b Kopeček J. Adv. Drug Deliv. Rev. 2013; 65:49. [PubMed: 23123294]
86. a Rösler A, Vandermeulen G, Klok HA. Adv. Drug Deliv. Rev. 2012; 64:270.b Zhang Q, Ko NR, Oh JK. Chem. Commun. 2012; 48:7542.
87. a Raemdonck K, Demeester J, De Smedt S. Soft Matter. 2009; 5:707.b Eckmann DM, Composto RJ, Tsourkas A, Muzykantov VR. J. Mater. Chem. B. 2014; 2:8085.
88. a Peer D, Karp JM, Hong S, Farokhzad OC, Margalit R, Langer R. Nat. Nanotechnol. 2007; 2:751. [PubMed: 18654426] b Davis ME, Chen ZG, Shin DM. Nat. Rev. Drug Discov. 2008; 7:771. [PubMed: 18758474] c Petros RA, DeSimone JM. Nat. Rev. Drug Discov. 2010; 9:615. [PubMed: 20616808]
89. a Chen Y, Wilbon PA, Zhou J, Nagarkatti M, Wang C, Chu F, Tang C. Chem. Commun. 2013; 49:297.b Li M, Tang Z, Sun H, Ding J, Song W, Chen X. Polym. Chem. 2013; 4:1199.
90. Azagarsamy MA, Alge DL, Radhakrishnan SJ, Tibbitt MW, Anseth KS. Biomacromolecules. 2012; 13:2219. [PubMed: 22746981]
91. Smith MH, Lyon LA. Acc. Chem. Res. 2012; 45:985. [PubMed: 22181582]
92. Li Y, Maciel D, Rodrigues J, Shi X, Tomas H. Chem. Rev. 2015; 115:8564. [PubMed: 26259712]
93. Liang Y, Kiick KL. Acta Biomater. 2014; 10:1588. [PubMed: 23911941]
94. a Wang D-A, Varghese S, Sharma B, Strehin I, Fermanian S, Gorham J, Fairbrother DH, Cascio B, Elisseeff JH. Nat. Mater. 2007; 6:385. [PubMed: 17435762] b Li F, Na K. Biomacromolecules. 2011; 12:1724. [PubMed: 21417397] c Murai T, Sougawa N, Kawashima H, Yamaguchi K, Miyasaka M. Immunol. Lett. 2004; 93:163. [PubMed: 15158613]
95. Yang X, Du H, Liu J, Zhai G. Biomacromolecules. 2015; 16:423. [PubMed: 25517794]
96. Zhang X, Malhotra S, Molina M, Haag R. Chem. Soc. Rev. 2015; 44:1948. [PubMed: 25620415]
97. Choi JH, Jang JY, Joung YK, Kwon MH, Park KD. J. Control. Release. 2010; 147:420. [PubMed: 20688114]
98. Joung YK, Jang JY, Choi JH, Han DK, Park KD. Mol. Pharm. 2013; 10:685. [PubMed: 23237335]
99. Yang HN, Choi JH, Park JS, Jeon SY, Park KD, Park K-H. Biomaterials. 2014; 35:4716. [PubMed: 24630837]
100. Nakai T, Hirakura T, Sakurai Y, Shimoboji T, Ishigai M, Akiyoshi K. Macromol. Biosci. 2012; 12:475. [PubMed: 22606703]
101. a Montanari E, Capece S, Di Meo C, Meringolo M, Coviello T, Agostinelli E, Matricardi P. Macromol. Biosci. 2013; 13:1185. [PubMed: 23836462] b Wei X, Senanayake TH, Warren G, Vinogradov SV. Bioconjugate Chem. 2013; 24:658.

102. a Jing J, Alaimo D, De Vlieghere E, Jérôme C, De Wever O, De Geest BG, Auzély-Velty R. J. Mater. Chem. B. 2013; 1:3883.b Stefanello, T. Fernandes; Szarpak-Jankowska, A.; Appaix, F.; Louage, B.; Hamard, L.; De Geest, BG.; van der Sanden, B.; Nakamura, CV.; Auzély-Velty, R. Acta Biomater. 2014; 10:4750. [PubMed: 25110287]
103. Park W, Park S-J, Na K. Colloids Surf. B. Biointerfaces. 2010; 79:501. [PubMed: 20541919]
104. Lim JJ, Hammoudi TM, Bratt-Leal AM, Hamilton SK, Kepple KL, Bloodworth NC, McDevitt TC, Temenoff JS. Acta Biomater. 2011; 7:986. [PubMed: 20965281]
105. Kabanov AV, Vinogradov SV. Angew. Chem. Int. Edit. 2009; 48:5418.
106. Zha L, Banik B, Alexis F. Soft Matter. 2011; 7:5908.
107. Sasaki Y, Akiyoshi K. Chem. Rec. 2010; 10:366. [PubMed: 20836092]
108. Yang C, Wang X, Yao X, Zhang Y, Wu W, Jiang X. J. Control. Release. 2015; 205:206. [PubMed: 25665867]
109. Wutzel H, Richter FH, Li Y, Sheiko SS, Klok H-A. Polym. Chem. 2014; 5:1711.
110. Xu X, Jha AK, Duncan RL, Jia X. Acta Biomater. 2011; 7:3050. [PubMed: 21550426]
111. Hettiaratchi MH, Miller T, Temenoff JS, Guldberg RE, McDevitt TC. Biomaterials. 2014; 35:7228. [PubMed: 24881028]
112. Xi J, Zhou L, Dai H. Colloids Surf. B. Biointerfaces. 2012; 100:107. [PubMed: 22771525]
113. Messager L, Portecop N, Hachet E, Lapeyre V, Pignot-Paintrand I, Catargi B, Auzély-Velty R, Ravaine V. J. Mater. Chem. B. 2013; 1:3369.
114. Zhang J, Gao W, Fang RH, Dong A, Zhang L. Small. 2015; 11:4309. [PubMed: 26044721]
115. Hachet E, Sereni N, Pignot-Paintrand I, Ravaine V, Szarpak-Jankowska A, Auzély-Velty R. J. Colloid. Interface. Sci. 2014; 419:52. [PubMed: 24491329]
116. a Meng F, Hennink WE, Zhong Z. Biomaterials. 2009; 30:2180. [PubMed: 19200596] b Cheng R, Feng F, Meng F, Deng C, Feijen J, Zhong Z. J. Control. Release. 2011; 152:2. [PubMed: 21295087]
117. Wu G, Fang Y-Z, Yang S, Lupton JR, Turner ND, Nutr J. 2004; 134:489.
118. a Lee H, Mok H, Lee S, Oh Y-K, Park TG. J. Control. Release. 2007; 119:245. [PubMed: 17408798] b Bae KH, Mok H, Park TG. Biomaterials. 2008; 29:3376. [PubMed: 18474396]
119. Nguyen DH, Choi JH, Joung YK, Park KD. J. Bioact. Compat. Pol. 2011; 26:287.
120. Pedrosa SS, Gonçalves C, David L, Gama M. Macromol. Biosci. 2014; 14:1556. [PubMed: 25088667]
121. Wu W, Yao W, Wang X, Xie C, Zhang J, Jiang X. Biomaterials. 2015; 39:260. [PubMed: 25468376]
122. a Rodell CB, Kaminski AL, Burdick JA. Biomacromolecules. 2013; 14:4125. [PubMed: 24070551] b Mealy JE, Rodell CB, Burdick JA. J. Mater. Chem. B. 2015; 3:8010.
123. Kim KS, Park SJ, Yang J-A, Jeon J-H, Bhang SH, Kim B-S, Hahn SK. Acta Biomater. 2011; 7:666. [PubMed: 20883838]
124. Patterson J, Hubbell JA. Biomaterials. 2010; 31:7836. [PubMed: 20667588]
125. Peattie RA, Nayate AP, Firpo MA, Shelby J, Fisher RJ, Prestwich GD. Biomaterials. 2004; 25:2789. [PubMed: 14962557]
126. a Wieland JA, Houchin-Ray TL, Shea LD. J. Control. Release. 2007; 120:233. [PubMed: 17582640] b Lei Y, Huang S, Sharif-Kashani P, Chen Y, Kavehpour P, Segura T. Biomaterials. 2010; 31:9106. [PubMed: 20822811]
127. Bian L, Zhai DY, Tous E, Rai R, Mauck RL, Burdick JA. Biomaterials. 2011; 32:6425. [PubMed: 21652067]
128. Jha AK, Malik MS, Farach-Carson MC, Duncan RL, Jia X. Soft Matter. 2010; 6:5045. [PubMed: 20936090]
129. Xiao L, Tong Z, Chen Y, Pochan DJ, Sabanayagam CR, Jia X. Biomacromolecules. 2013; 14:3808. [PubMed: 24093583]
130. a Ekaputra AK, Prestwich GD, Cool SM, Hutmacher DW. Biomaterials. 2011; 32:8108. [PubMed: 21807407] b Bhakta G, Rai B, Lim ZXH, Hui JH, Stein GS, van Wijnen AJ, Nurcombe V, Prestwich GD, Cool SM. Biomaterials. 2012; 33:6113. [PubMed: 22687758]

131. a Purcell BP, Kim IL, Chuo V, Guenin T, Dorsey SM, Burdick JA. Biomater. Sci. 2014; 2:693. [PubMed: 24955239] b Scharnweber D, Hübner L, Rother S, Hempel U, Anderegg U, Samsonov SA, Pisabarro MT, Hofbauer L, Schnabelrauch M, Franz S, Simon J, Hintze V. J. Mater. Sci.-Mater. Med. 2015; 26:232. [PubMed: 26358319]
132. Hudalla GA, Murphy WL. Adv. Funct. Mater. 2011; 21:1754. [PubMed: 21921999]
133. Zieris A, Prokoph S, Levental KR, Welzel PB, Grimmer M, Freudenberg U, Werner C. Biomaterials. 2010; 31:7985. [PubMed: 20674970]
134. Freudenberg U, Sommer J-U, Levental KR, Welzel PB, Zieris A, Chwalek K, Schneider K, Prokoph S, Prewitz M, Dockhorn R, Werner C. Adv. Funct. Mater. 2012; 22:1391.
135. Prokoph S, Chavakis E, Levental KR, Zieris A, Freudenberg U, Dimmeler S, Werner C. Biomaterials. 2012; 33:4792. [PubMed: 22483246]
136. Schurig K, Zieris A, Hermann A, Freudenberg U, Heidel S, Grimmer M, Storch A, Werner C. Biomaterials. 2015; 67:205. [PubMed: 26222283]
137. Watarai A, Schirmer L, Thönes S, Freudenberg U, Werner C, Simon JC, Anderegg U. Acta Biomater. 2015; 25:65. [PubMed: 26219861]
138. Tsurkan MV, Hauser PV, Zieris A, Carvalhosa R, Bussolati B, Freudenberg U, Camussi G, Werner C. J. Control. Release. 2013; 167:248. [PubMed: 23395667]
139. Zieris A, Chwalek K, Prokoph S, Levental KR, Welzel PB, Freudenberg U, Werner C. J. Control. Release. 2011; 156:28. [PubMed: 21763368]
140. Shulman JM, De Jager PL, Feany MB. Annu. Rev. Pathol. Mech. Dis. 2011; 6:193.
141. Carmeliet P. Nature. 2005; 438:932. [PubMed: 16355210]
142. Pike DB, Cai S, Pomraning KR, Firpo MA, Fisher RJ, Shu XZ, Prestwich GD, Peattie RA. Biomaterials. 2006; 27:5242. [PubMed: 16806456]
143. Ding X, Gao J, Awada H, Wang Y. J. Mater. Chem. B. 2016; 4:1175.
144. Schächinger V, Erbs S, Elsässer A. N. Engl. J. Med. 2006; 355:1210. [PubMed: 16990384]
145. Urbich C, Dimmeler S. Circ. Res. 2004; 95:343. [PubMed: 15321944]
146. Baumann L, Prokoph S, Gabriel C, Freudenberg U, Werner C, Beck-Sickinger AG. J. Control. Release. 2012; 162:68. [PubMed: 22634073]
147. Bellomo R, Kellum JA, Ronco C. Lancet. 2012; 380:756. [PubMed: 22617274]
148. Zimmermann R, Bartsch S, Freudenberg U. Anal. Chem. 2012; 84:9592. [PubMed: 23030581]
149. Humes HD, Cieslinski DA, Coimbra TM, Messana JM, Galvao C. J. Clin. Invest. 1989; 84:1757. [PubMed: 2592559]
150. Singer AJ, Clark RA. N. Engl. J. Med. 1999; 341:738. [PubMed: 10471461]
151. Liu Y, Cai S, Shu XZ, Shelby J, Prestwich GD. Wound Repair Regen. 2007; 15:245. [PubMed: 17352757]
152. Petitou M, Hérault J-P, Bernat A, Driguez P-A, Duchaussoy P, Lormeau J-C, Herbert J-M. Nature. 1999; 398:417. [PubMed: 10201371]
153. Takano R. Trends Glycosci. Glyc. 2002; 14:343.
154. Zieris A, Dockhorn R, Röhrich A, Zimmermann R, Müller M, Welzel PB, Tsurkan MV, Sommer J-U, Freudenberg U, Werner C. Biomacromolecules. 2014; 15:4439. [PubMed: 25329425]
155. Freudenberg U, Zieris A, Chwalek K, Tsurkan MV, Maitz MF, Atallah P, Levental KR, Eming SA, Werner C. J. Control. Release. 2015; 220:79. [PubMed: 26478015]
156. Krieger JR, Ogle ME, McFaline-Figueroa J, Segar CE, Temenoff JS, Botchwey EA. Biomaterials. 2016; 77:280. [PubMed: 26613543]
157. a Lutolf MP. P. Natl. Acad. Sci. USA. 2003; 100:5413.b Lutolf MP, Hubbell JA. Biomacromolecules. 2003; 4:713. [PubMed: 12741789]
158. Chwalek K, Tsurkan MV, Freudenberg U, Werner C. Sci. Rep. 2014; 4:4414. [PubMed: 24643064]
159. Bray LJ, Binner M, Holzheu A, Friedrichs J, Freudenberg U, Hutmacher DW, Werner C. Biomaterials. 2015; 53:609. [PubMed: 25890757]
160. Ferdowsian HR, Gluck JP. Camb. Q. Healthc. Ethics. 2015; 24:391. [PubMed: 26364775]
161. Gojgini S, Tokatlian T, Segura T. Mol. Pharm. 2011; 8:1582. [PubMed: 21823632]

162. Lam J, Carmichael ST, Lowry WE, Segura T. Adv. Healthc. Mater. 2015; 4:534. [PubMed: 25378176]
163. Lam J, Segura T. Biomaterials. 2013; 34:3938. [PubMed: 23465825]
164. Lam J, Lowry WE, Carmichael ST, Segura T. Adv. Funct. Mater. 2014; 24:7053. [PubMed: 26213530]
165. Zhu S, Nih L, Carmichael ST, Lu Y, Segura T. Adv. Mater. 2015; 27:3620. [PubMed: 25962336]
166. Wen J, Anderson SM, Du J, Yan M, Wang J, Shen M, Lu Y, Segura T. Adv. Mater. 2011; 23:4549. [PubMed: 21910141]
167. Cam C, Zhu S, Truong NF, Scumpia PO, Segura T. J. Mater. Chem. B Mater. Biol. Med. 2015; 3:7986. [PubMed: 26509037]
168. Cam C, Segura T. Curr. Opin. Biotech. 2013; 24:855. [PubMed: 23680305]
169. Lei Y, Rahim M, Ng Q, Segura T. J. Control. Release. 2011; 153:255. [PubMed: 21295089]
170. Purcell BP, Lobb D, Charati MB, Dorsey SM, Wade RJ, Zellars KN, Doviak H, Pettaway S, Logdon CB, Shuman JA, Freels PD, Gorman JH III, Gorman RC, Spinale FG, Burdick JA. Nat. Mater. 2014; 13:653. [PubMed: 24681647]
171. a Yamaguchi N, Zhang L, Chae B-S, Palla CS, Furst EM, Kiick KL. J. Am. Chem. Soc. 2007; 129:3040. [PubMed: 17315874] b Kim SH, Kiick KL. Macromol. Rapid Commun. 2010; 31:1231. [PubMed: 21567519]
172. Dahlbäck B. Lancet. 2000; 355:1627. [PubMed: 10821379]
173. Maitz MF, Freudenberg U, Tsurkan MV, Fischer M, Beyrich T, Werner C. Nat. Commun. 2013; 4:2168. [PubMed: 23868446]
174. Guerrini M, Beccati D, Shriver Z, Naggi A, Viswanathan K, Bisio A, Capila I, Lansing JC, Guglieri S, Fraser B, Al-Hakim A, Gunay NS, Zhang Z, Robinson L, Buhse L, Nasr M, Woodcock J, Langer R, Venkataraman G, Linhardt RJ, Casu B, Torri G, Sasisekharan R. Nat. Biotechnol. 2008; 26:669. [PubMed: 18437154]
175. a Seeberger PH, Werz DB. Nature. 2007; 446:1046. [PubMed: 17460666] b Seeberger PH. Chem. Soc. Rev. 2008; 37:19. [PubMed: 18197330]
176. Eller S, Collot M, Yin J, Hahm HS, Seeberger PH. Angew. Chem. Int. Edit. 2013; 52:5858.
177. Kandasamy J, Schuhmacher F, Hahm HS, Klein JC, Seeberger PH. Chem. Commun. 2014; 50:1875.
178. Seeberger, PH. New Chemistry and New Opportunities from the Expanding Protein Universe. Wüthrich, K.; Hilvert, D., editors. New Jersey, USA: 2014. Ch. 3
179. Farrugia B, Lord M, Melrose J, Whitelock J. Molecules. 2015; 20:4254. [PubMed: 25751786]
180. Lim D-K, Wylie RG, Langer R, Kohane DS. Biomaterials. 2016; 77:130. [PubMed: 26588795]
181. Salbach-Hirsch J, Samsonov SA, Hintze V, Hofbauer C, Picke A-K, Rauner M, Gehrcke J-P, Moeller S, Schnabelrauch M, Scharnweber D, Pisabarro MT, Hofbauer LC. Biomaterials. 2015; 67:335. [PubMed: 26232882]
182. Boltje TJ, Buskas T, Boons GJ. Nature Chem. 2009; 1:611. [PubMed: 20161474]
183. a Xu Y, Masuko S, Takieddin M, Xu H, Liu R, Jing J, Mousa SA, Linhardt RJ, Liu J. Science. 2011; 334:498. [PubMed: 22034431] b Masuko S, Linhardt RJ. Future Med. Chem. 2012; 4:289. [PubMed: 22393937] c Liu J, Linhardt RJ. Nat. Prod. Rep. 2014; 31:1676. [PubMed: 25197032]
184. Sterner E, Masuko S, Li G, Li L, Green DE, Otto NJ, Xu Y, DeAngelis PL, Liu J, Dordick JS, Linhardt RJ. J. Biol. Chem. 2014; 289:9754. [PubMed: 24563485]
185. Multhaupt HAB, Couchman JR. J. Histochem. Cytochem. 2012; 60:908. [PubMed: 22899865]
186. Suflita M, Fu L, He W, Koffas M, Linhardt RJ. Appl. Microbiol. Biotechnol. 2015; 99:7465. [PubMed: 26219501]
187. a Ranga A, Gobaa S, Okawa Y, Mosiewicz K, Negro A, Lutolf MP. Nat. Comms. 2014; 5:4324.b Ranga A, Lutolf MP. Curr. Opin. Cell Biol. 2012; 24:236. [PubMed: 22301436] c Cosson S, Lutolf MP. Sci. Rep. 2014; 4:4462. [PubMed: 24662945] d Kobel S, Lutolf MP. Curr. Opin. Biotech. 2011; 22:690. [PubMed: 21821410]
188. Fischbach C, Chen R, Matsumoto T, Schmelzle T, Brugge JS, Polverini PJ, Mooney DJ. Nat. Meth. 2007; 4:855.

189. a Lee K, Silva EA, Mooney DJ. J. R. Soc. Interface. 2011; 8:153. [PubMed: 20719768] b Vo TN, Kasper FK, Mikos AG. Adv. Drug Deliv. Rev. 2012; 64:1292. [PubMed: 22342771]

190. a Sun Q, Silva EA, Wang A, Fritton JC, Mooney DJ, Schaffler MB, Grossman PM, Rajagopalan S. Pharm. Res. 2010; 27:264. [PubMed: 19953308] b Yilgor P, Tuzlakoglu K, Reis RL, Hasirci N, Hasirci V. Biomaterials. 2009; 30:3551. [PubMed: 19361857] c Chen F-M, Zhang M, Wu Z-F. Biomaterials. 2010; 31:6279. [PubMed: 20493521]

191. a Baumann MD, Kang CE, Stanwick JC, Wang Y, Kim H, Lapitsky Y, Shoichet MS. J. Control. Release. 2009; 138:205. [PubMed: 19442692] b Appel EA, Tibbitt MW, Webber MJ, Mattix BA, Veiseh O, Langer R. Nat. Commun. 2015; 6:6295. [PubMed: 25695516] c Awada HK, Johnson NR, Wang Y. J. Control. Release. 2015; 207:7. [PubMed: 25836592] d Wickremasinghe NC, Kumar VA, Shi S, Hartgerink JD. ACS Biomater. Sci. Eng. 2015; 1:845. [PubMed: 26925462] e Liang Y, Kiick KL. Biomacromolecules. 2016; 17:601. [PubMed: 26751084]

192. Azagarsamy MA, Anseth KS. Angew. Chem. Int. Edit. 2013; 52:13803.

193. Belair DG, Le NN, Murphy WL. Chem. Commun. 2014; 50:15651.

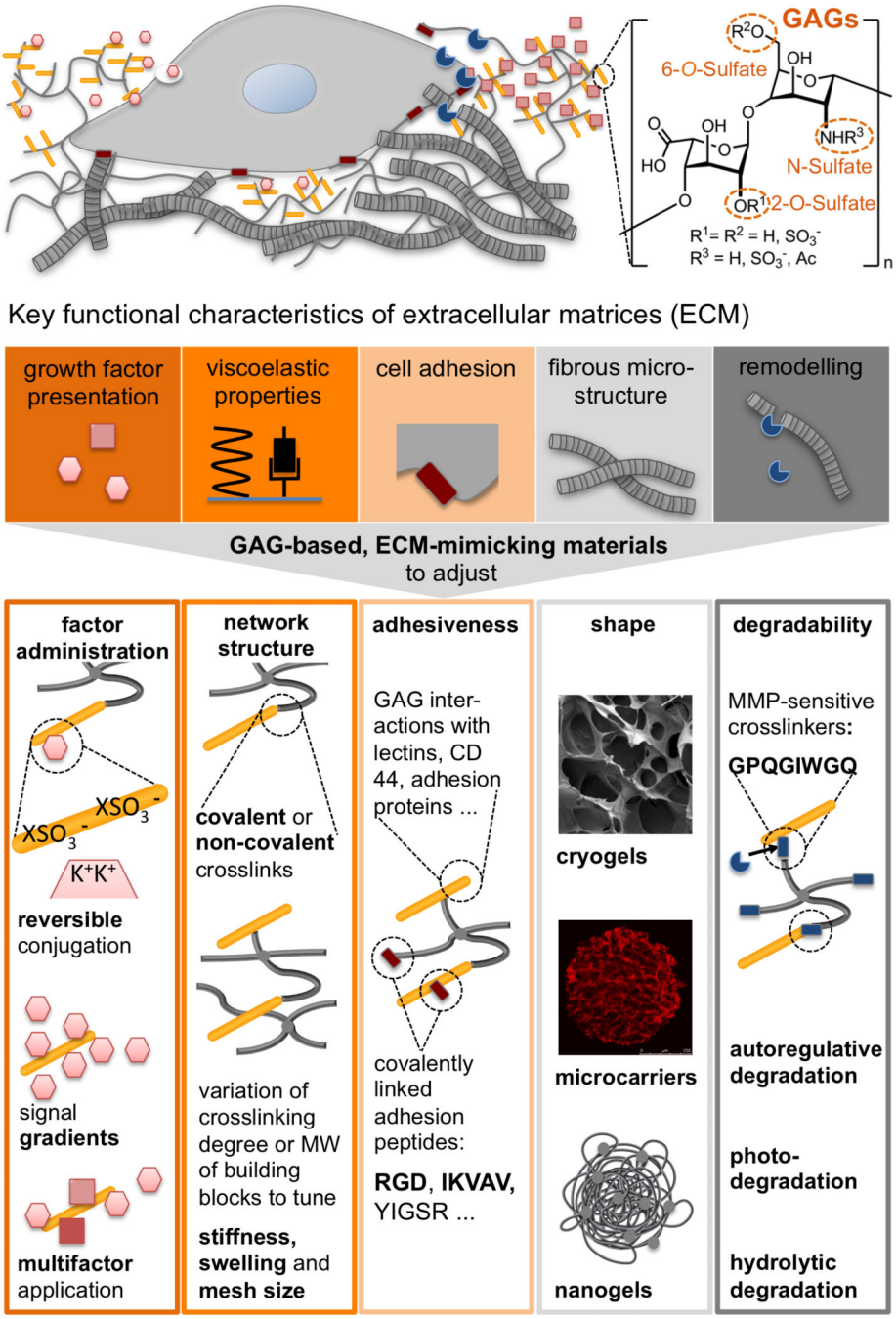

Figure 1.

Top: Cell-instructive characteristics of the extracellular matrix (ECM) governing tissue formation, homeostasis and regeneration. Glycosaminoglycans (GAGs) with different sulfation patterns are a main component of the ECM (orange). The ECM affords adaptable physical properties (viscoelastic properties, black) with structural heterogeneity (grey), allows cell-responsive remodeling (blue), displays adhesion ligands/attachment sites (red) and modulates morphogen signaling (light red). Bottom: GAG-based biomaterials can be instrumental in recapitulating these fundamental ECM features through the molecular design

and processing of polymer networks to tune the administration of soluble factors, the network structure, the adhesiveness, the shape and the degradability of the matrices respectively.

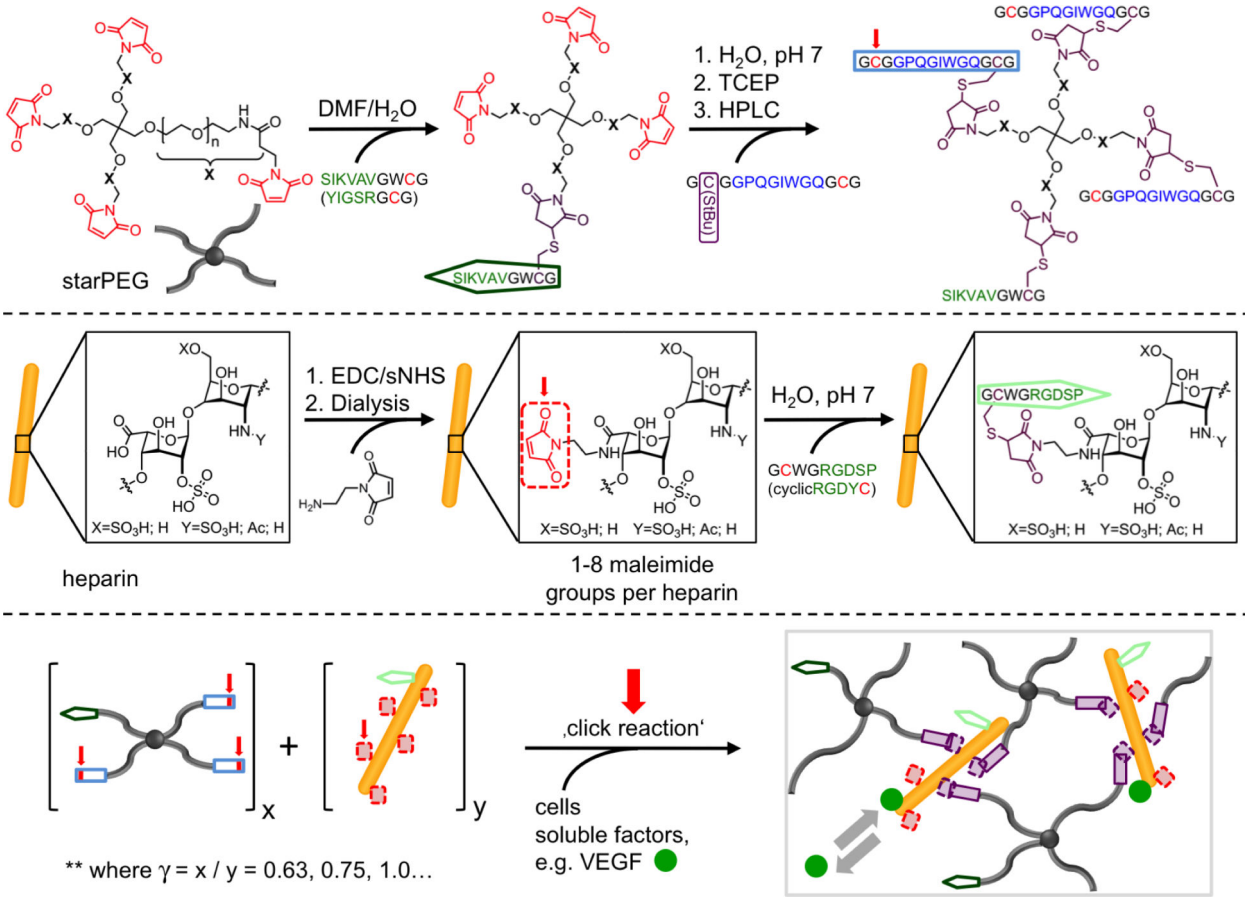

Figure 2.

Synthetic scheme for the in situ formation of multifunctional starPEG-HEP-peptide hydrogels. Reaction partners/reactive moieties are highlighted in red, cell adhesion receptor-binding proteins are highlighted in green, and MMP-responsive crosslinking peptides are highlighted in blue. Reproduced with permission from Ref. [28], copyright (2013) Wiley.

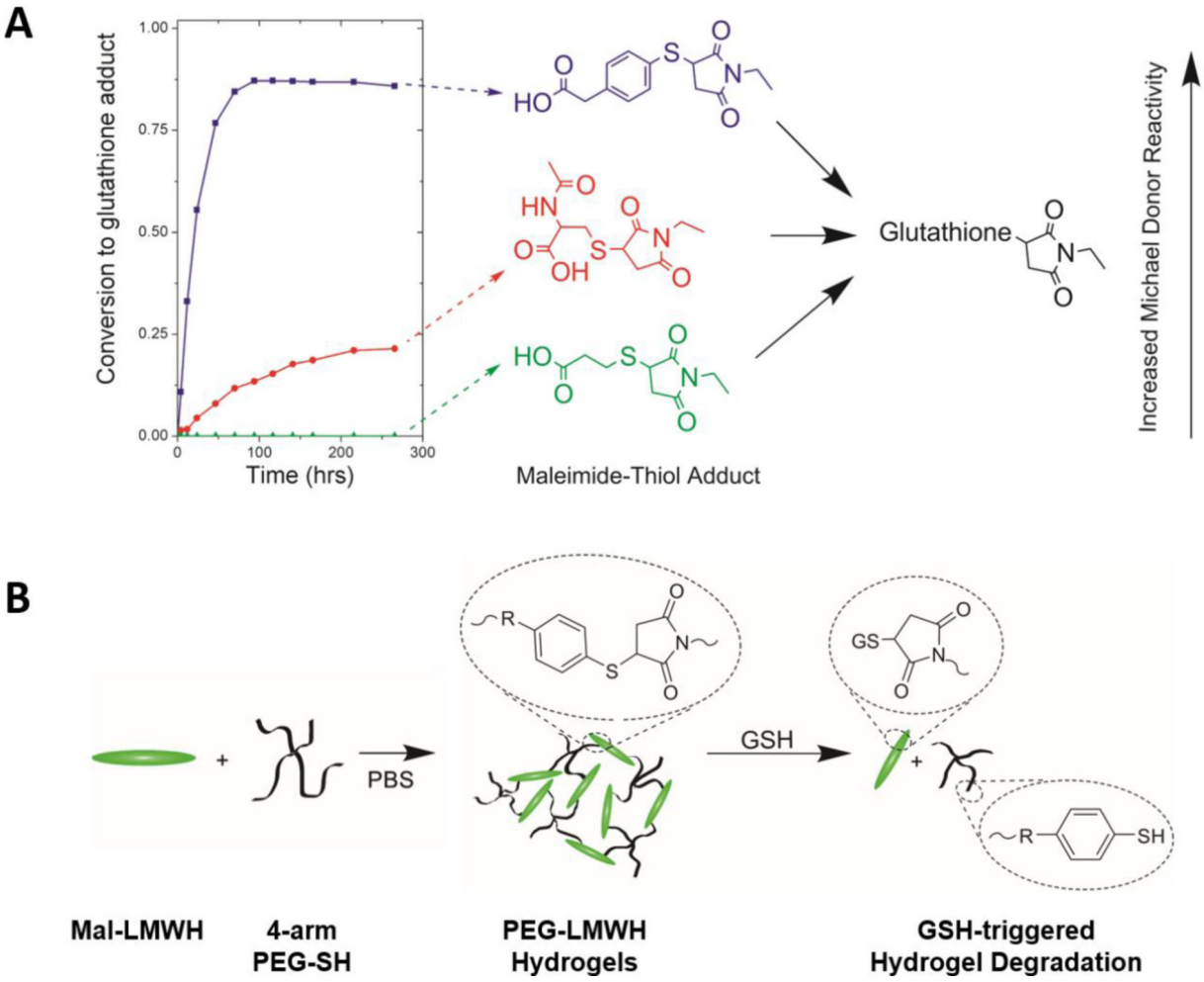

Figure 3.

Reduction-sensitive degradation of PEG-low-molecular-weight HEP (LMWHEP) hydrogels via a reversible thiol-maleimide Michael-type addition. A) Conversion of retro-Michael adducts formed with Michael donors of different reactivity. B) Schematic representation of the formation and degradation of GSH-responsive PEG-LMWH(EP) hydrogels. Reproduced with permission from Ref.[53] (A), copyright (2011) American Chemical Society and adapted with permission from Ref.[52] (B), copyright (2013) The Royal Society of Chemistry.

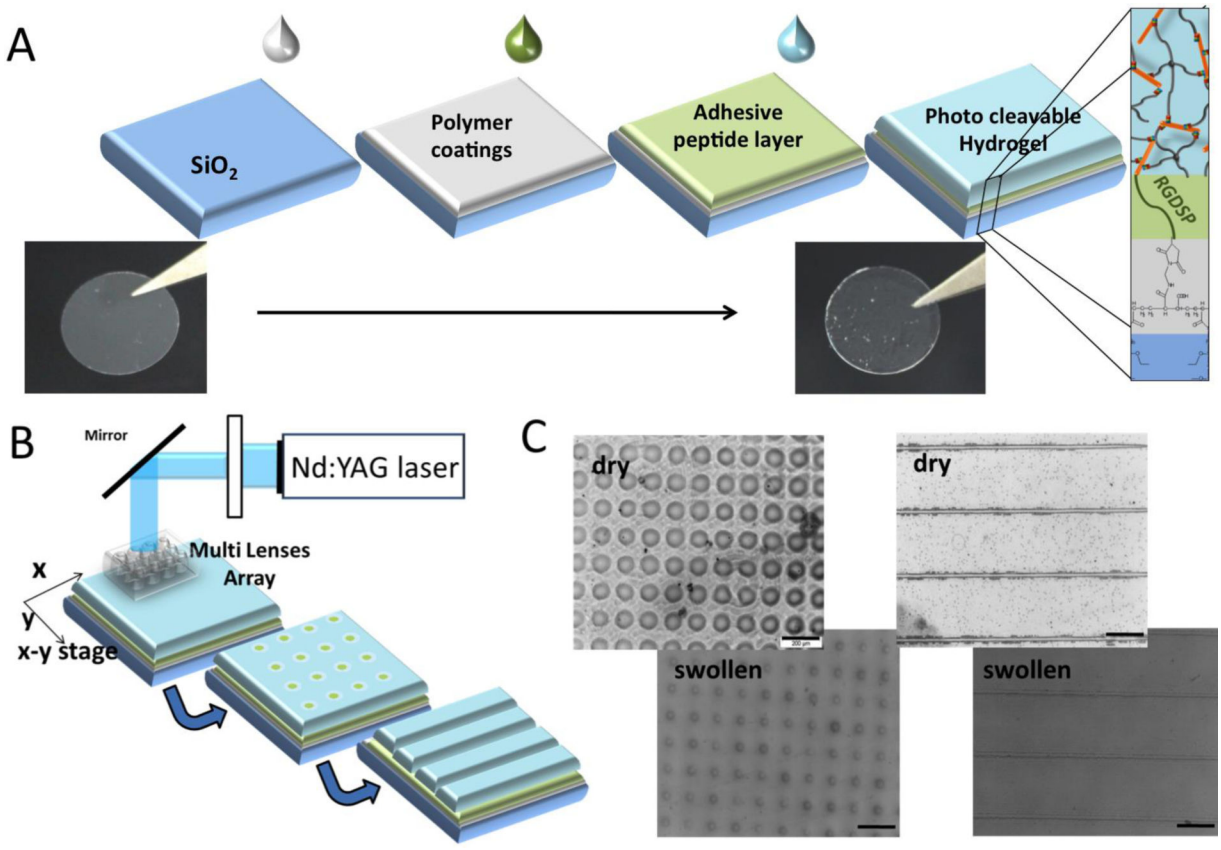

Figure 4.

Photopatterning of PEG-HEP hydrogels to direct adult neural precursor cells. A) Schematic view of the formation of the multilayer coating on glass. B) Schematic view of the hydrogel structure using the Micro Lens array and 355 nm laser light. C) Light microscopy images of the hydrogel well and channel patterns in the dry and swollen states (scale bar = 200 μm). Reproduced with permission from Ref.[58], copyright (2015) John Wiley & Sons.

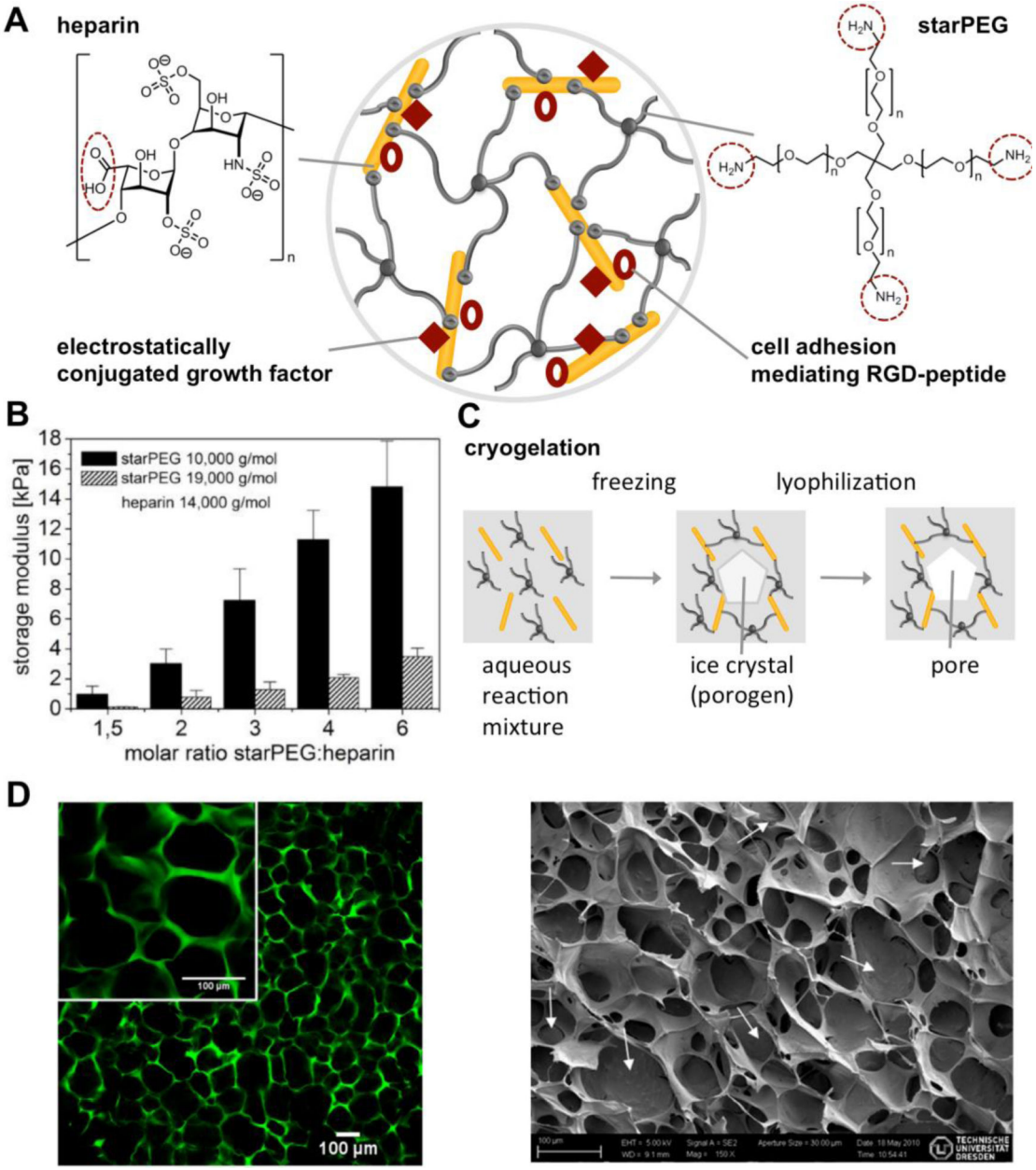

Figure 5.

Biohybrid starPEG-HEP hydrogels. A) Schematic drawing of a hydrogel crosslinked via amide bond formation between amine-terminated starPEG and carboxylic acid groups of HEP (red dotted circles), allowing the subsequent covalent conjugation of adhesion peptides and the reversible biomimetic conjugation of morphogens. B) Variation of the mechanical properties of the hydrogels by altering the molar ratio of the building blocks (■) and the molecular weight of the starPEG building block, reproduced from[61] with permission from MDPI, Basel, Switzerland. C) Cryogelation of similar starPEG-HEP hydrogels using ice crystal formation as a porogen, followed by a lyophilization step to create interconnected micropores. D) Left: Confocal laser scanning micrograph of Alexa® 488 (green)-labeled

cryogels swollen in phosphate-buffered saline. Right: Scanning electron micrograph of a dry cryogel, reproduced with permission from[63], copyright ACS Publications 2012.

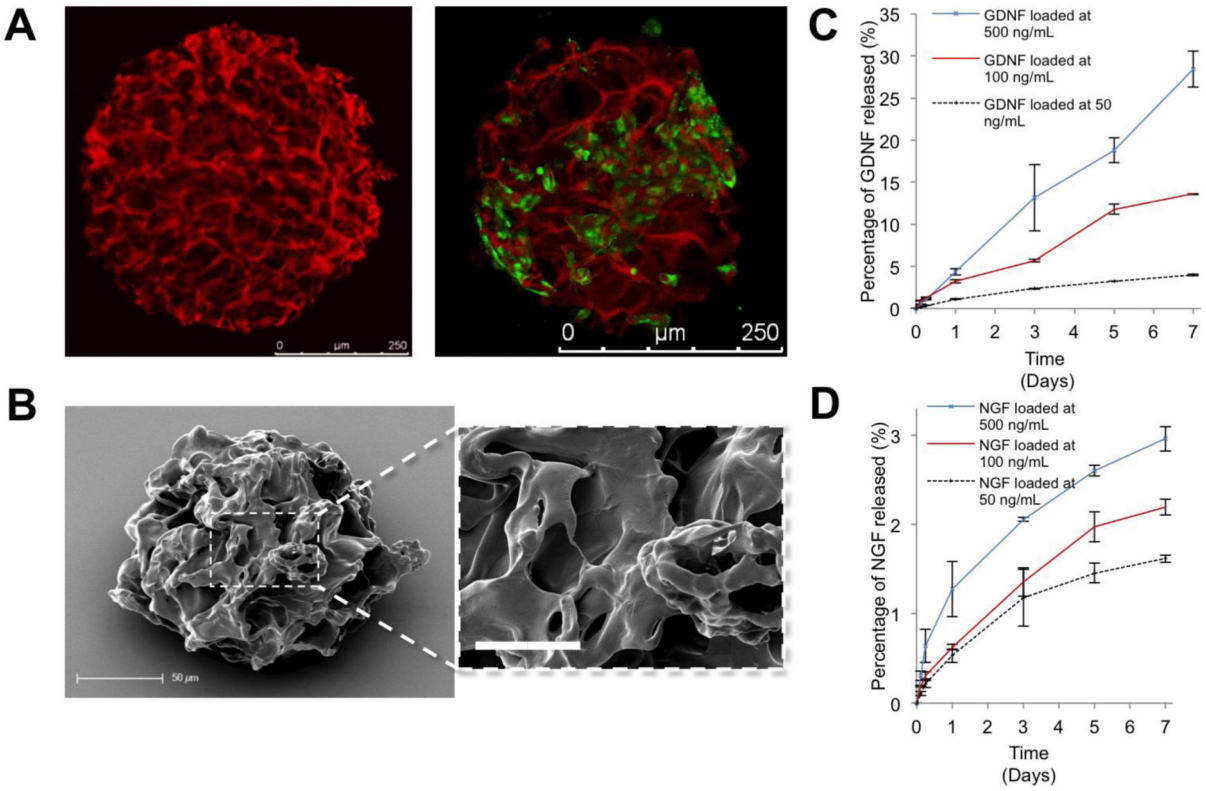

Figure 6.

Shape-memory cryogel microcarriers formed from starPEG-HEP hydrogels with interconnected porosity. A) Left: Confocal laser scanning micrograph of Alexa® 647 (red)-labeled cryogels swollen in phosphate-buffered saline. Right: GFP-positive mesenchymal stem cell (green) grown on cryogel particles (red). B) Scanning electron micrograph of a dry cryogel microparticle showing the pore structure and high magnification insert, scale bar: 20 µm C) GDNF and D) NGF release into the medium from the microcarriers is tunable by altering the initial loading concentration. Reproduced with permission from Ref.[67], copyright (2013) Wiley.

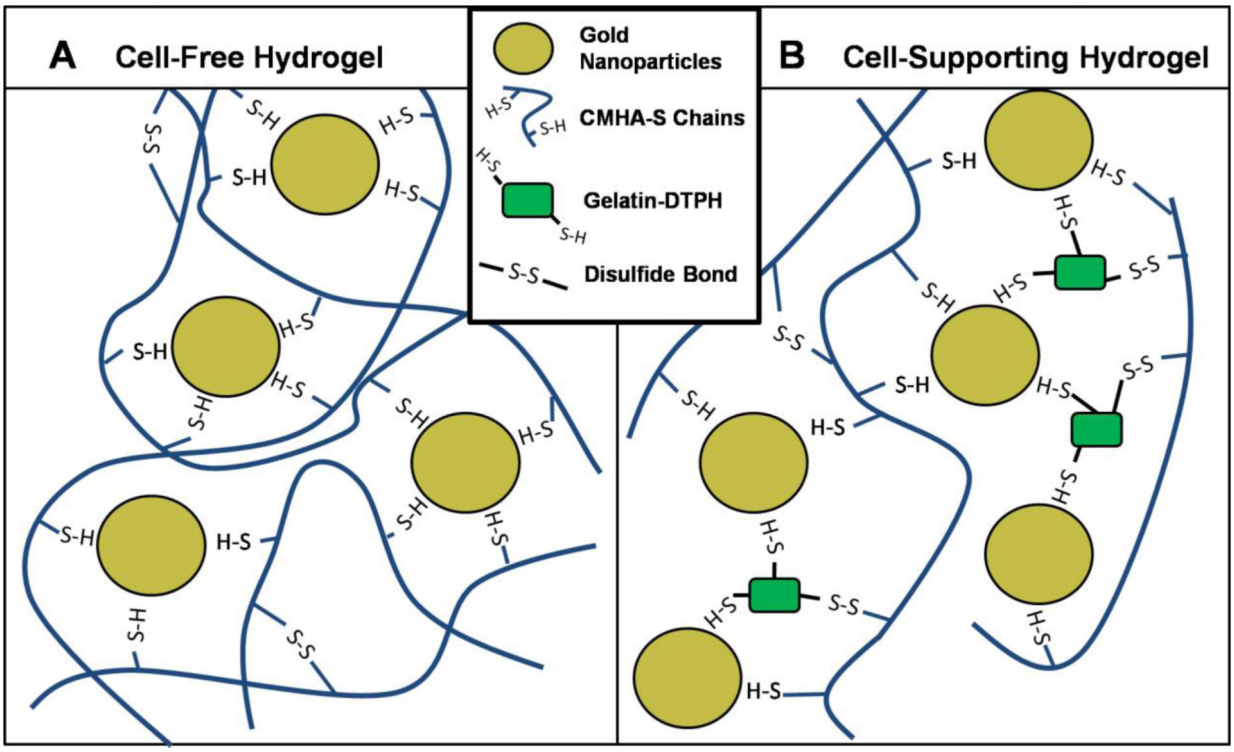

Figure 7.

Multivalent gold nanoparticle (AuNP) crosslinkers form bonds with thiols depicted on thiol-modified HA (CMHA-S) and thiol-modified gelatin (Gtn-DTPH), creating a network. In (A), AuNP-CMHA-S gels lack cell attachment factors, while in (B), AuNP-CMHA-S-Gtn-DTPH gels support cell attachment (not to scale). Reproduced with permission from Ref. [84], copyright (2010) Wiley.

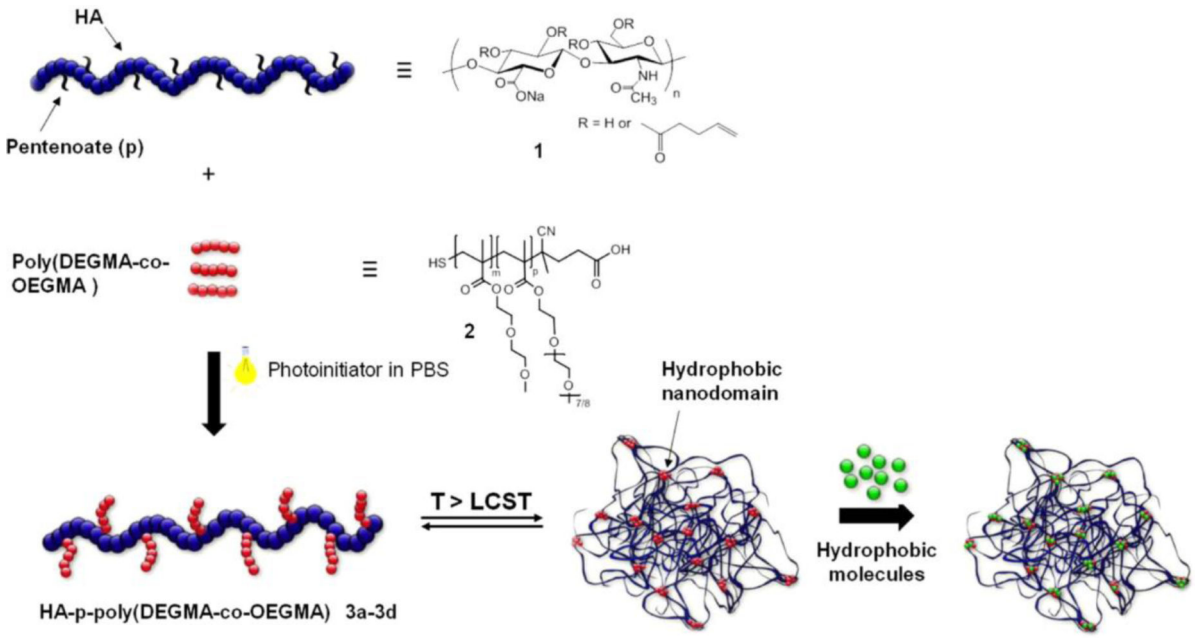

Figure 8.

Formation of thermoresponsive HA nanogels. HA was modified with the thermoresponsive copolymers poly(DEGMA-co-OEGMA) via thiol-ene chemistry, allowing temperature-triggered assembly into nanogels and the facile encapsulation of hydrophobic molecules. Reproduced with permission from Ref.[102b], copyright (2014) Elsevier.

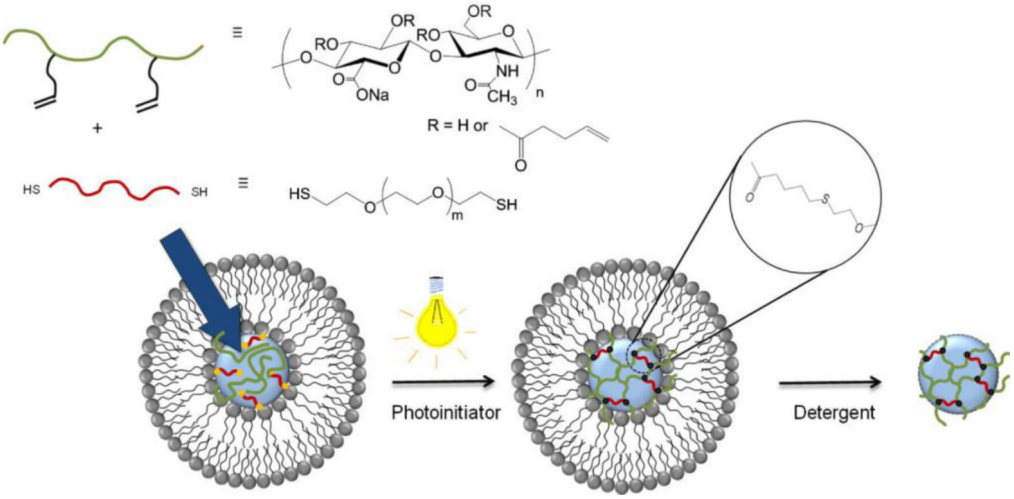

Figure 9.

Synthesis of chemically crosslinked HA nanogels via the use of liposome templates in aqueous solutions. Liposomes encapsulating HA-pentenoate, PEG-$(SH)_2$ and Irgacure 2959 were exposed to UV light to trigger the crosslinking of HA by thiol-ene chemistry. HA nanogels were obtained after the subsequent removal of the lipid bilayers. Reproduced with permission from Ref.[115], copyright (2014) Elsevier.

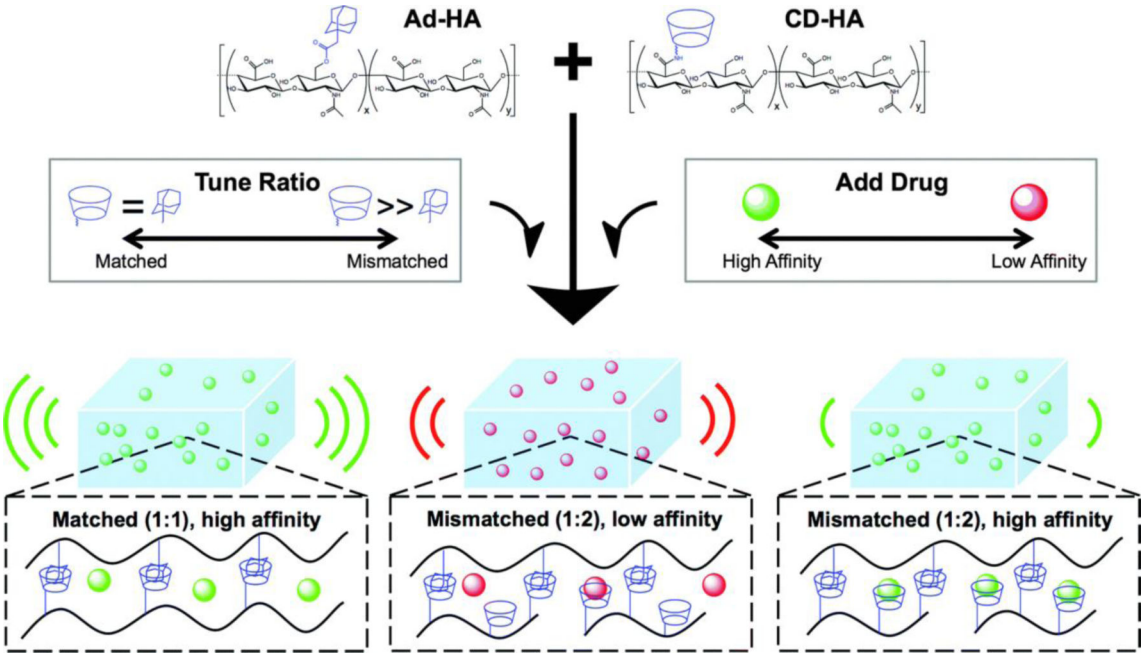

Figure 10.

Tunable release of various small molecules from supramolecular HA hydrogels prepared using Ad-HA and CD-HA macromers. Macromers were dissolved in solutions containing various drugs (green = high affinity for CD, red = low affinity for CD) and combined in varying ratios (Ad : CD) to produce bulk hydrogels. Release kinetics were tuned by varying the CD content available for drug binding or by altering the affinity of the loaded drug for CD. Reproduced with permission from Ref.[122b], copyright (2015) The Royal Society of Chemistry.

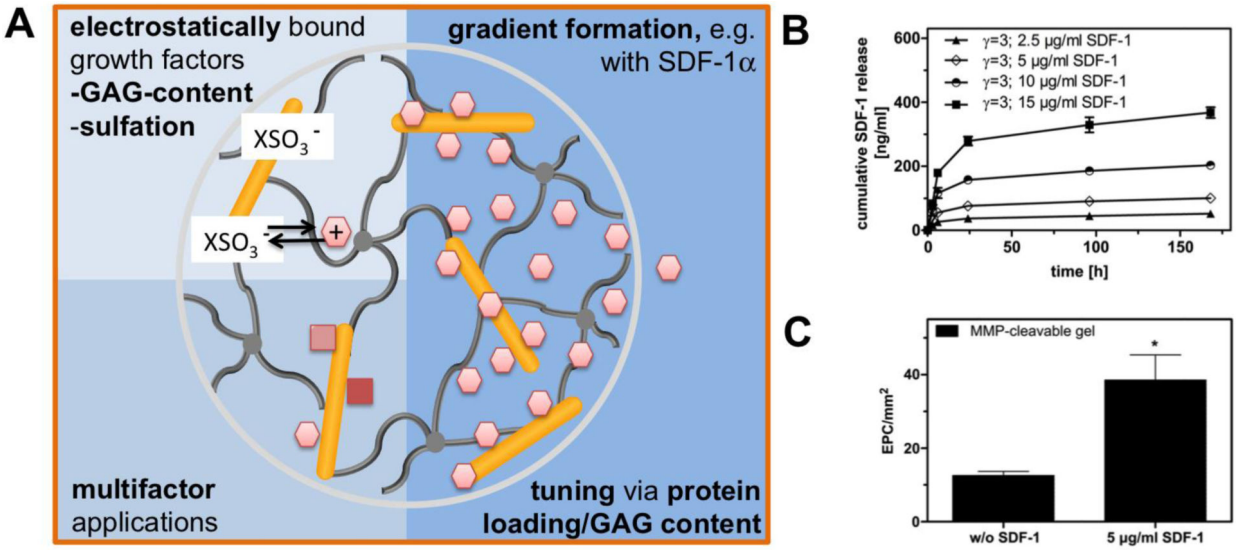

Figure 11.

Administration of growth factors from GAG-based hydrogels utilizing electrostatic interactions. A) Schematic drawing of the interplay between growth factors displaying positively charged amino acid residues and the sulfate groups of GAGs, allowing multifactor applications and long-lasting morphogen concentration gradients. B) The cumulative release and gradient formation of SDF-1α from starPEG-HEP matrices is tunable by varying the initial loading concentration. C) The subcutaneous implantation of SDF-1α-loaded starPEG-HEP hydrogels increased the number of EPCs homing to the tissue. The number of EPCs present in the hydrogel after 48 h of implantation was quantified. The data are presented as the means ± standard error of the mean from n = 4-5 (*indicates $p<0.05$ versus control without SDF-1α; ANOVA). Adapted with permission from Ref.[135], copyright (2012) Elsevier.

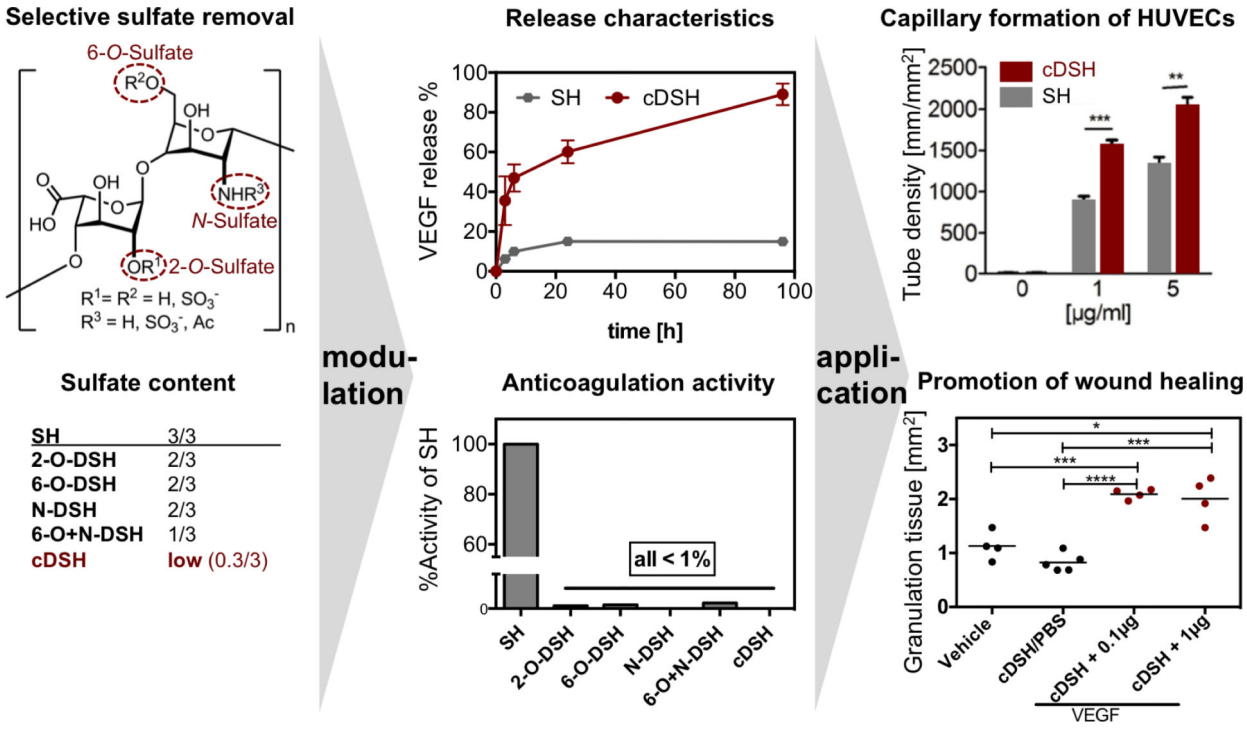

Figure 12.

StarPEG-HEP hydrogels with variable sulfation patterns. Left: Selectively desulfated HEP was used as a building block for biohybrid starPEG-HEP hydrogels. Middle - modulation (top): Cumulative VEGF release from HEP (SH) and completely desulfated HEP (cDSH) hydrogels, expressed as percent immobilization; (bottom): Anticoagulant activity of desulfated HEP derivatives compared to standard HEP. Right - application (top): Quantification of the tube length of HUVECs on a collagen I/starPEG-HEP gel sandwich after 3 days of culture; (bottom) StarPEG-HEP hydrogels promoted wound angiogenesis in diabetic mice. Morphometric quantification of granulation tissue was performed after 10 days. Adapted with permission from Ref.[155], copyright (2015) Elsevier.

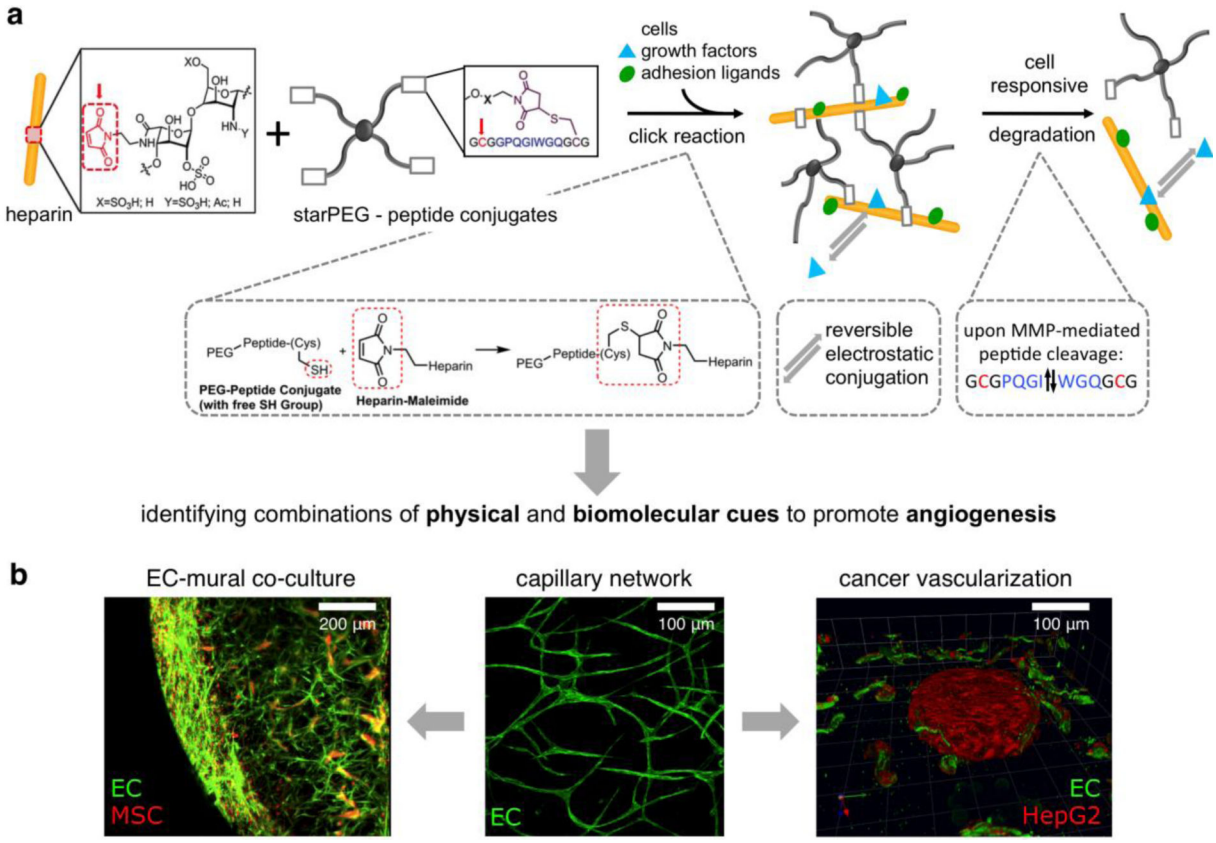

Figure 13.

MMP-degradable starPEG-HEP hydrogels as an extracellular milieu to study heterotypic cell-cell interactions during angiogenic events. A) Hydrogels prepared using MMP-cleavable peptide linkers via a Michael-type addition allow the in situ encapsulation of growth factors and cells as well as cell-responsive degradation. B) The MMP-degradable mechanism of the matrix creates a cell-responsive environment for EC capillary formation, enabling the exploration of vascular capillary stabilization by mural cells and tumor vascularization. Reproduced with permission from Ref.[158], copyright (2014) Nature Publishing Group.

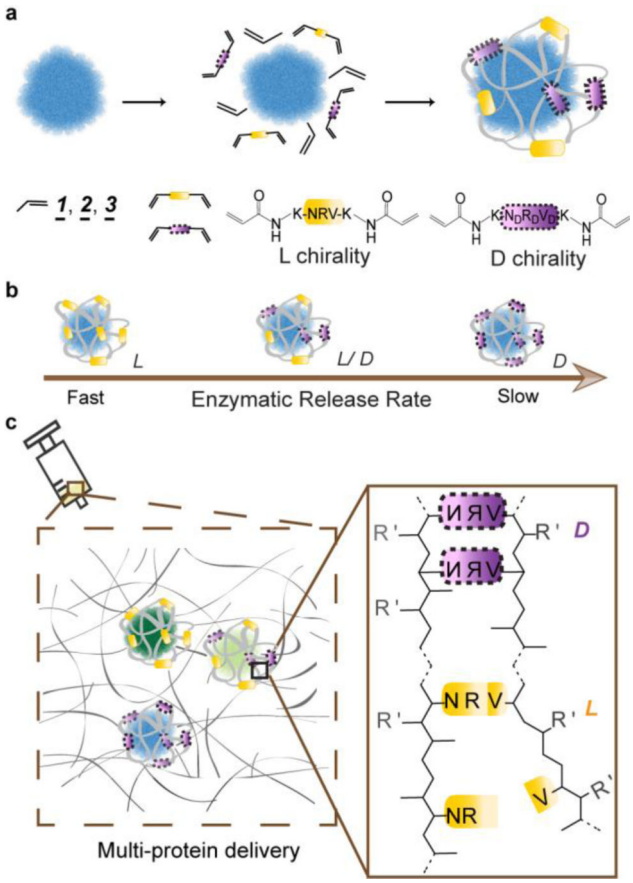

Figure 14.

Protease-degradable growth factor nanocapsules protect growth factors during hydrogel formation and control the release of growth factors *in vitro* and *in vivo*. Growth factor nanocapsules are formed through the in situ radical polymerization of acrylate and acrylamide-containing monomers and peptide crosslinkers to generate a hydrated nanohydrogel shell around a single protein. The result is a single protein nanocapsule that is protease degradable through the incorporated peptide crosslinkers. The speed of degradation is modulated by introducing D peptide sequences that are degraded more slowly by the proteases. Reproduced with permission from Ref.[165] copyright (2015) Wiley.

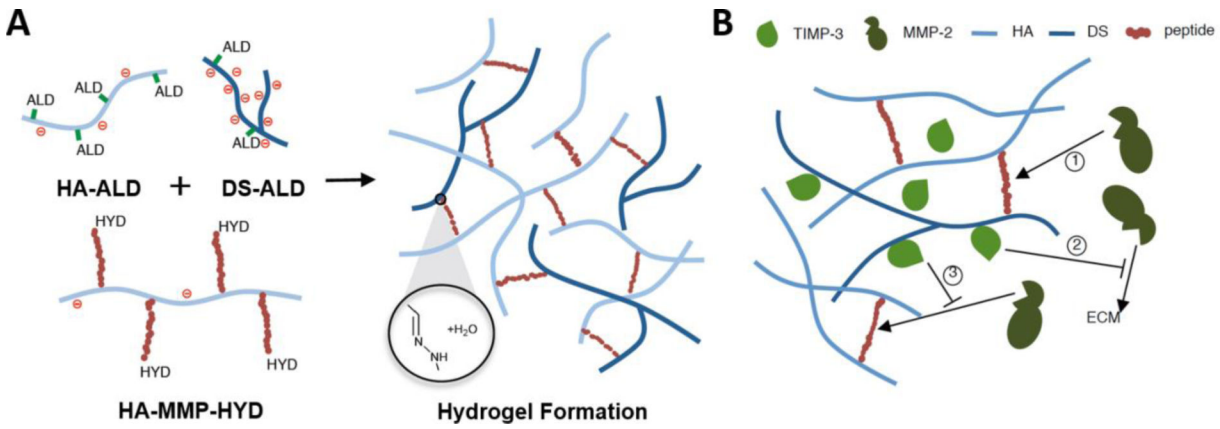

Figure 15.

Injectable and cell-responsive HA hydrogels for on-demand matrix metalloproteinase inhibition. A) Hydrogel crosslinking was designed through hydrazone bond formation between complementary aldehyde (ALD) and hydrazine (HYD) groups to form hydrogels under physiologic conditions. Dextran sulfate (DS) was incorporated into the network to act as an HEP mimetic to immobilize encapsulated HEP-binding rTIMP-3. B) In this hydrogel system, MMPs degrade the hydrogel crosslinks (1), liberating polysaccharide-bound rTIMP-3, which then inhibits local MMP activity (2) and attenuates further hydrogel degradation (3). Reproduced with permission from Ref.[170], copyright (2014) Nature Publishing Group.

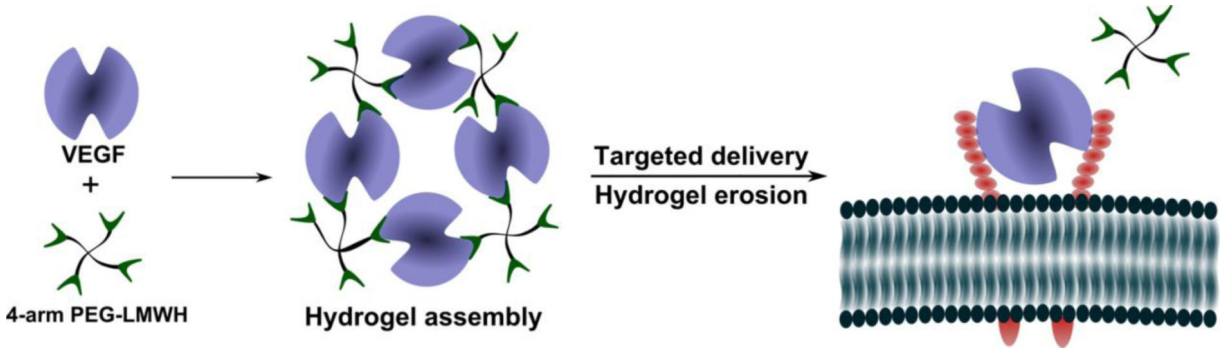

Figure 16.

Cell-mediated delivery and targeted erosion of growth factor-crosslinked hydrogels. Non-covalently assembled hydrogels were formed by the crosslinking of polysaccharide-derivatized star copolymers by dimeric HEP-binding growth factors. The receptor-mediated erosion of the hydrogels enabled the cell-responsive targeted delivery of VEGF. Reproduced with permission from Ref.[171b], copyright (2010) John Wiley & Sons.

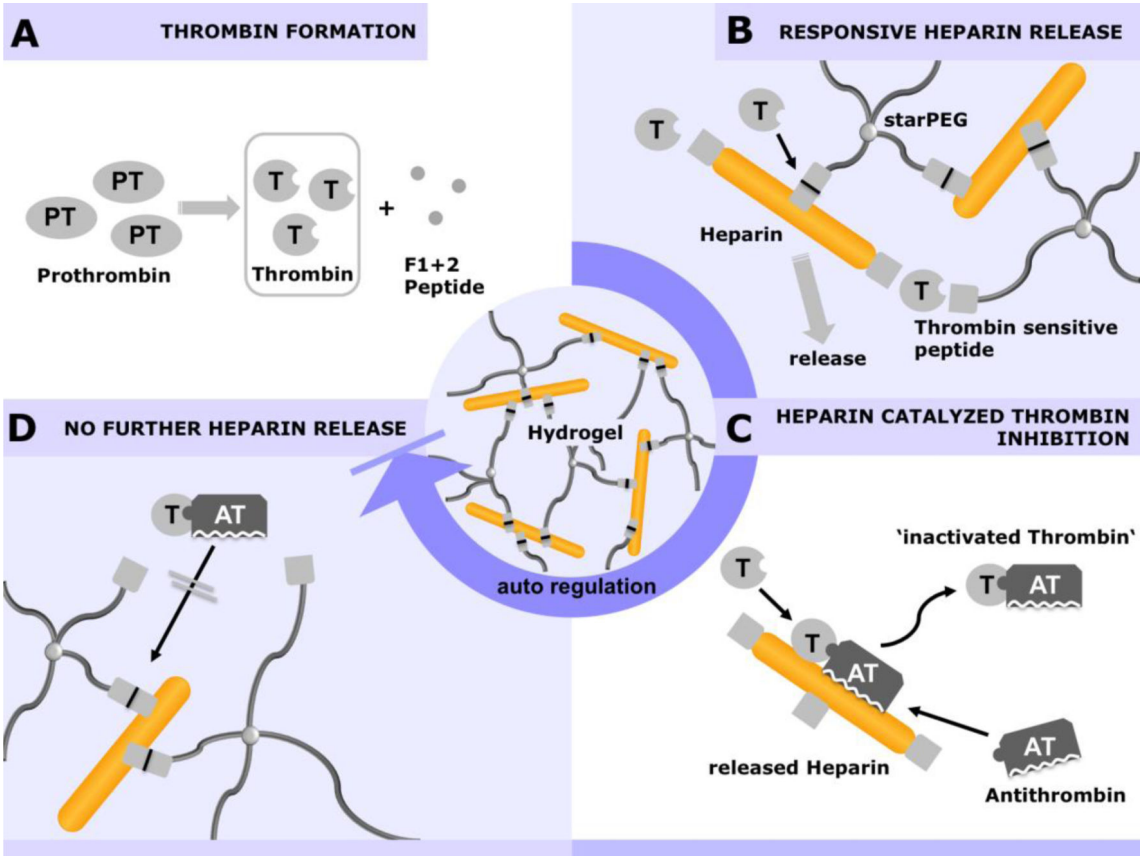

Figure 17.

Autoregulation of HEP release from thrombin-sensitive starPEG-HEP hydrogels. A) Activated thrombin, originating from various activation pathways linked to the exposure of blood to foreign materials, carries the risk of subsequent thrombus formation. B) The thrombin selectively cleaves the peptide of the linker unit in the starPEG-HEP and releases HEP with kinetics that depend on the degree of crosslinking. C) The released HEP catalyzes the complexation of thrombin with its plasma-based inhibitor antithrombin, resulting in the inactivation of thrombin and D) cessation of further hydrogel degradation. Reproduced with permission from Ref.[173], copyright (2013) Nature Publishing Group.

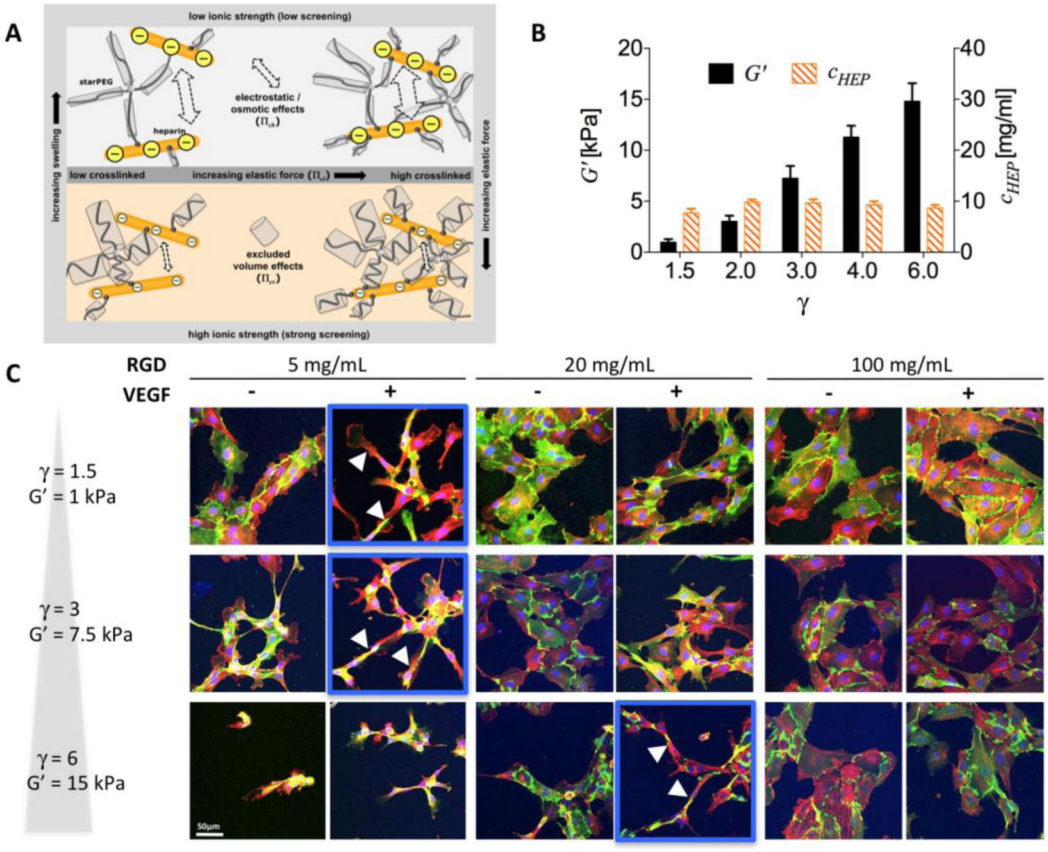

Figure 18.

A) Rationally designed starPEG-HEP hybrid networks. The interplay among elastic forces (Π_{el}) (~crosslinking degree), excluded volume (Π_{ev}), and electrostatic/osmotic effects (Π_{ch}) was evaluated while maintaining the swelling and HEP concentration of the swollen matrices ($\Pi_{el} = \Pi_{ch} + \Pi_{el}$). B) Constant HEP concentration and variable storage moduli (experimental) in swollen networks, as predicted by the mean field approach. C) HUVECs form a network of tube-like structures (arrows indicate cells with a high aspect ratio) in hydrogels with independently tunable VEGF and RGD functionalization and storage moduli. Immunofluorescence images of CD31 (green; endothelial cell marker), actin (red), and DAPI (blue) in HUVECs plated for 20–24 h are representative of the results from 3 independent experiments. Reproduced with permission from Ref.[134], copyright (2012) Wiley.

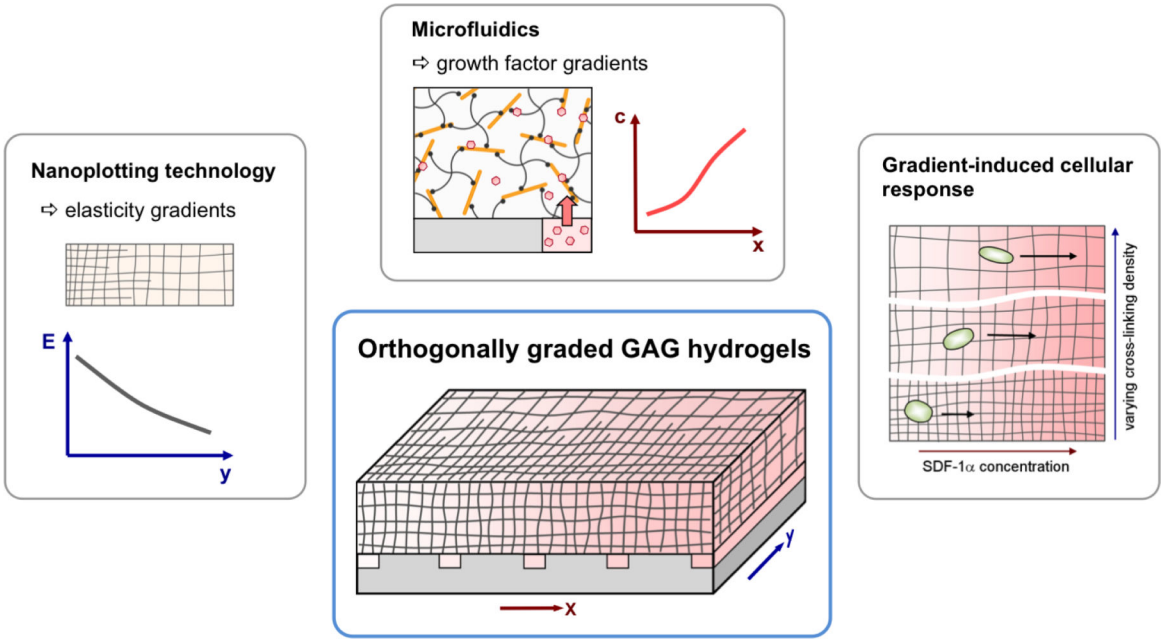

Figure 19.

Combinatorial approach involving nanoplotting technology, microfluidics and customized GAG synthesis to design orthogonally graded exogenous cues for high-throughput screening of cellular response patterns.